



Brookhaven
National Laboratory

BNL-101496-2014-TECH

AD/AP 6;BNL-101496-2013-IR

Nonlinear effects and chromaticity studies for the AGS booster

Z. Parsa

June 1987

Collider Accelerator Department
Brookhaven National Laboratory

U.S. Department of Energy

USDOE Office of Science (SC)

Notice: This technical note has been authored by employees of Brookhaven Science Associates, LLC under Contract No. DE-AC02-76CH00016 with the U.S. Department of Energy. The publisher by accepting the technical note for publication acknowledges that the United States Government retains a non-exclusive, paid-up, irrevocable, world-wide license to publish or reproduce the published form of this technical note, or allow others to do so, for United States Government purposes.

DISCLAIMER

This report was prepared as an account of work sponsored by an agency of the United States Government. Neither the United States Government nor any agency thereof, nor any of their employees, nor any of their contractors, subcontractors, or their employees, makes any warranty, express or implied, or assumes any legal liability or responsibility for the accuracy, completeness, or any third party's use or the results of such use of any information, apparatus, product, or process disclosed, or represents that its use would not infringe privately owned rights. Reference herein to any specific commercial product, process, or service by trade name, trademark, manufacturer, or otherwise, does not necessarily constitute or imply its endorsement, recommendation, or favoring by the United States Government or any agency thereof or its contractors or subcontractors. The views and opinions of authors expressed herein do not necessarily state or reflect those of the United States Government or any agency thereof.

AD/AP/Tech. Note No. 6

Accelerator Development Department

BROOKHAVEN NATIONAL LABORATORY
Associated Universities, Inc.
Upton, New York 11973

Accelerator Physics Technical Note. No. 6

NONLINEAR EFFECTS AND CHROMATICITY STUDIES FOR THE AGS BOOSTER

Zohreh Parsa

June 1987

BROOKHAVEN NATIONAL LABORATORY
UPTON, NEW YORK 11973

NONLINEAR EFFECTS AND CHROMATICITY STUDIES FOR THE AGS BOOSTER

ZOHREH PARSA

This is a summary of the presentation at the April and May 1987 (Interdepartmental) Accelerator Physics seminars at the Physics Department. It includes a theoretical overview of our formalism¹ and some results of our chromaticity studies for the operation of the Booster. Comparison of our analytic results and those obtained from program HARMON and tracking programs PATRICIA (F. Dell) and ORBIT (G. Parzen) are also included.

I. Theory (an overview)

II. AGS Booster

II. THEORY

The Hamiltonian of a dynamical system can be expressed by

$$H = \frac{2\pi}{C} v_x^0 J_x + \frac{2\pi}{C} v_z^0 J_z + V(J_x, J_z, \phi_x, \phi_z, s) \quad (1)$$

where (J_x, ϕ_x) and (J_z, ϕ_z) are the action - angle variables; v_x^0 and v_z^0 are the linear tunes; C is the circumference of the machine and V (the perturbing potential) is periodic in ϕ_x , ϕ_z , and s.

Expanding V in a fourier series about ϕ_x , ϕ_z , and s, we find a term in which the argument of the Sine and Cosine term varies the slowest with s. Since this term gives the greatest contribution to the dynamics of the system, we only consider this term and neglect the others. This leads to the following Hamiltonian:

$$\begin{aligned} H \approx & \frac{2\pi}{C} v_x^0 J_x + \frac{2\pi}{C} v_z^0 J_z + I(J_x, J_z) \\ & + \frac{1}{C} A(J_x, J_z) \cos(n_x \phi_x + n_z \phi_z - \frac{2\pi}{C} ps + \theta) \end{aligned} \quad (2)$$

Where $A(J_x, J_z)$ is the Hamiltonian Resonance strength, θ is the constant phase and $I(J_x, J_z)$ is the term that causes the perturbation of tune, p, n_x and n_z defines a given resonance.

To find the resonance strengths, we make a canonical transformation of the Hamiltonian Eq. (2) with the generating function of the form:

$$G(K_x, K_z, \phi_x, \phi_z, s) = K_x \phi_x + K_z \phi_z + \sum_k \frac{g_k(K_x, K_z, s)}{\sin \pi (n_{x_k} v_x + n_{z_k} v_z)} \cos(n_{x_k} \phi_x + n_{z_k} \phi_z + \theta_k) \quad (3)$$

$$\sum_k \frac{g_k(K_x, K_z, s)}{\sin \pi (n_{x_k} v_x + n_{z_k} v_z)} \cos(n_{x_k} \phi_x + n_{z_k} \phi_z + \theta_k)$$

Where $g_k(K_x, K_z, s)$ are the generating function resonance strengths whose magnitude shows to what extent J_x and J_z deviate from the invariants of the motion. The n_{x_k} and n_{z_k} are integers defining a given resonance and θ_k are the phase.

The new Hamiltonian can be found from the generating function as;

$$H_2 = H_1 (J_x, J_z, \phi_x, \phi_z, s) + \frac{\partial}{\partial s} G (K_x, K_z, \phi_x, \phi_z, s) \quad (4)$$

with

$$J_x = \frac{\partial}{\partial \phi_x} G (K_x, K_z, \phi_x, \phi_z, s) \quad (5)$$

$$= E_x / 2\pi$$

$$J_z = \frac{\partial}{\partial \phi_z} G (K_x, K_z, \phi_x, \phi_z, s)$$

$$= E_z / 2\pi \quad (6)$$

and the new angle variables;

$$\psi_x = \frac{\partial}{\partial K_x} G (K_x, K_z, \phi_x, \phi_z, s) \quad (7)$$

$$\psi_z = \frac{\partial}{\partial K_z} G (K_x, K_z, \phi_x, \phi_z, s) \quad (8)$$

With K_x , K_z , ψ_x and ψ_z as the new action and angle variables respectively

$$\begin{aligned} \psi_x &= \phi_x + \sum_k \left[\frac{\partial}{\partial K_x} g_k (K_x, K_z, s) \cos(n_{x_k} \phi_x + n_{z_k} \phi_z \right. \\ &\quad \left. + \theta_k) - g_k (K_x, K_z, s) \frac{\partial}{\partial K_x} \theta_k (K_x, K_z, s) \sin(n_{x_k} \phi_x + \right. \\ &\quad \left. n_{z_k} \phi_z + \theta_k) \right] \frac{1}{\sin(\pi(n_{x_k} v_x + n_{z_k} v_z))} \end{aligned} \quad (9)$$

and

$$\begin{aligned}
\psi_z &= \phi_z + \sum_k \frac{\partial}{\partial K_z} g_k(K_x, K_z, s) \cos(n_{x_k} \phi_x + n_{z_k} \phi_z \\
&\quad + \theta_k) - g_k(K_x, K_z, s) \frac{\partial}{\partial K_z} \theta_k(K_x, K_z, s) \sin(n_{x_k} \phi_x \\
&\quad + n_{z_k} \phi_z + \theta_k)] \frac{1}{\sin(\pi(n_{x_k} v_x + n_{z_k} v_z))} \tag{10}
\end{aligned}$$

Thus the perturbation on the tune due to the nonlinear elements (e.g. sextupoles and octupoles) can be found as

$$\frac{d}{ds} \psi_x(s) = \frac{\partial H}{\partial K_x} \tag{11}$$

$$\frac{d}{ds} \psi_x = \frac{1}{\beta_x(s)} + 2a(s) K_x + b(s) K_z$$

and

$$v_x \equiv \frac{1}{2\pi} \int_0^C [\frac{d}{ds} \psi_x(s)] ds$$

or

$$v_x = v_x^0 + 2a_{xx} K_x + 2a_{xz} K_z \tag{12}$$

Similarly,

$$\text{where } v_z = v_z^0 + 2a_{zz} K_z + 2a_{xz} K_x \tag{13}$$

$$a_{xx} = 1/\pi \int_0^C a(t) dt, a_{xz} = \frac{1}{2\pi} \int_0^C b(t) dt$$

with

$$a_{zz} = 1/\pi \int_0^C c(t) dt$$

Where the coefficients $a(s)$, $b(s)$ and $c(s)$ are given in Reference 1, and the machine tunes v_x and v_z depends on the beam emittance. The v_x^0 and v_z^0 are the unperturbed tunes and $2K_x$, $2K_z$ are proportional to the average beam emittances divided by π , $\langle E_x \rangle$ and $\langle E_z \rangle$ and

$$v_x^o = \frac{1}{2\pi} \int_0^C \frac{dt}{\beta_x(t)}$$

$$v_z^o = \frac{1}{2\pi} \int_0^C \frac{dt}{\beta_z(t)}$$

Thus we find the emittance growth to be

$$E_x \leq 2\pi \left[K_x + \sum_k n_{x_k} \left| \frac{g_k(K_x, K_z, s)}{\sin \pi (n_{x_k} v_x + n_{z_k} v_z)} \right| \right] \quad (14)$$

$$E_z \leq 2\pi \left[K_z + \sum_k n_{z_k} \left| \frac{g_k(K_x, K_z, s)}{\sin \pi (n_{x_k} v_x + n_{z_k} v_z)} \right| \right] \quad (15)$$

These estimate the upper limit that emittance grow to as long as the tunes are far from any resonances

Further, we can deduce the contribution of a single resonance to the emittance growth:

$$E_x = 2\pi \left[K_x + n_x \frac{a(K_x, K_z)}{\delta} \cos(n_x \phi_x + n_z \phi_z - \frac{2\pi}{C} ps + \theta) \right] \quad (16)$$

$$E_z = 2\pi \left[K_z + n_z \frac{a(K_x, K_z)}{\delta} \cos(n_x \phi_x + n_z \phi_z - \frac{2\pi}{C} ps + \theta) \right] \quad (17)$$

with $n_x > 0$ when $n_z < 0$ for difference resonances. The emittance oscillates about its average value (with oscillation amplitude proportional to $g(J_x, J_z) = a(J_x, J_z) / \delta$), where δ is the bandwidth (e.g. $\delta = 0$ near resonance) defined as

$$\delta \equiv n_x v_x + n_z v_z - p \quad (18)$$

which determines how far the tunes v_x and v_z are from the resonance (defined by integers n_x , n_z and p).

SMEAR

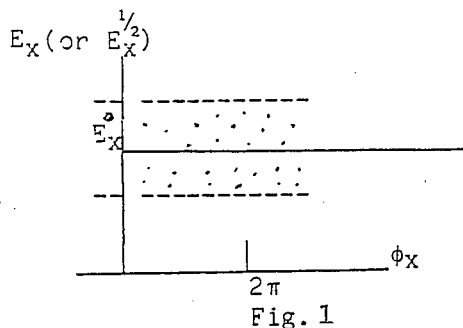
To find the "smear" (that is, the measure of the extent to which the emittance deviates from an invariant of the motion) we consider the variation of the emittance with respect to the time variable of the Hamiltonian s . The coefficients of equations (14 + 17), which are periodic functions of s , ϕ_x and ϕ_z ; can be expressed as functions of s times the sine and cosine of $(n_x \phi_x + n_z \phi_z)$. Then keeping ϕ_x and ϕ_z fixed, the emittance is periodic in s :

$$E_x (\phi_x, \phi_z, K_x, K_z, s) = E_x (\phi_x, \phi_z, K_x, K_z, s + C), \quad (19)$$

$$E_z (\phi_x, \phi_z, K_x, K_z, s) = E_z (\phi_x, \phi_z, K_x, K_z, s + C) \quad (20)$$

Where C is the circumference of the accelerator.

Note that, as we increase s by C then to the lowest order ϕ_x increases by $2\pi v_x$ and ϕ_z increases by $2\pi v_z$. Thus, overall E_x and E_z does not remain periodic in s if we include the ϕ_x and ϕ_z dependence of s . From the phase plots of E_x (or $E_z^{1/2}$) versus ϕ_x Fig. 1 we note that, if we had no non-linear elements all the points would fall on the line $E_x = E_{x0}$ (Ave E_x).



Since the nonlinear elements cause the deviation from this line, we can find the measure of this deviation from the "standard deviation" $D(E_x)$ which is related to the emittance as $D(E_x) = \text{smear}^{1/2}$, where smear is defined from the standard deviation of $E_x^{1/2}$.

$$D(E_x^{1/2}) = \text{smear} = \left[\frac{\sigma_x^2 + \sigma_z^2}{\langle E_x^{1/2} \rangle^2 + \langle E_z^{1/2} \rangle^2} \right]^{1/2}$$

where $\sigma_x = \langle E_x \rangle - \langle E_x^{1/2} \rangle^2$ and $\sigma_z = \langle E_z \rangle - \langle E_z^{1/2} \rangle^2$ or

$$\text{smear} = \left[\frac{\langle E_x \rangle + \langle E_z \rangle}{\langle E_x^{1/2} \rangle^2 + \langle E_z^{1/2} \rangle^2} - 1 \right]^{1/2}$$

and as a simpler alternative, the smear can be defined as:

$$\text{Smear}_x \approx \frac{1}{\sqrt{3}} \frac{E_x(\max) - E_x(\min)}{\langle E_x \rangle} = \frac{1}{\sqrt{3}} |n_x g(J_x, J_z)| \quad (21)$$

$$\text{Smear}_z \approx \frac{1}{\sqrt{3}} \frac{E_z(\max) - E_z(\min)}{\langle E_z \rangle} = \frac{1}{\sqrt{3}} |n_z g(J_x, J_z)| \quad (22)$$

Which are useful for obtaining the resonance coupling strength $g(J_x, J_z)$, (e.g. from the tracking results).

LINEAR APERTURE

We obtain the linear aperture a from $a = \sqrt{\beta_{\max} E_0 / \pi}$, where β_{\max} is the maximum betatron amplitude and E_0 is the initial beam emittance which gives a smear of 0.1.

Finally in our analysis of the beam behavior versus chromaticity (ξ) we consider

$$\xi_{x(\text{or } z)} = \frac{1}{4\pi} \int_0^C (-K(s) \pm S(s) D(s)) \beta_{x(\text{or } z)} ds \quad (23)$$

with $K(s)$ the quadrupole focusing strength, $S(s)$ is the sextupole strength (including Focusing, Defocusing and Eddy current in one case and sextupoles due to saturation in the second case respectively). Where $D(s)$ is the horizontal dispersion and $\beta(s)$ is the betatron function.

Thus, we first calculate the sextupole strengths in order to obtain the desired chromaticity then using second order perturbation theory we study the effect of the sextupoles (e.g. due to eddy current, chromatic correction and saturation) on the beam. In addition we compare the ordinary perturbation theory with the superconvergent perturbation theory, illustrating the amplitude dependence of the tune due to nonlinear elements in an accelerator.

AGS-BOOSTER

Due to the interest and request for more information on the Booster (during my April '87 talk) I first give an overview of the AGS Booster (the Parameter List) and a comparison of our analytic results (for the Booster) with results obtained from program HARMON and tracking programs PATRICIA and ORBIT.

The AGS-Booster is designed to be an intermediate synchrotron injector for the AGS with the capability of accelerating protons from 200 MeV to 1.5 GeV (with the possibility of an upgrade to 2.5 GeV), and capable of accelerating heavy ions to a magnetic rigidity equal to 17.52 Tesla meters at a 1 Hz repetition rate. The Booster has six identical superperiods and circumference of 201.78m; with an operating point at $v_x=4.82$ and $v_z=4.83$. The goal for the Booster is to increase the AGS proton and polarized proton intensities (by factors of 4 and 20 (to 30) respectively) in addition to enabling the acceleration of all species of heavy ions at the AGS. To increase the number of particles per bunch in the AGS, we need a high intensity beam in the Booster which may produce a large space charge tune shift in the Booster at injection. That space charge tune shift can use crossing of the fourth order structure resonances $4v_x=18$, $2v_x+2v_z=18$ and $4v_z=18$; (and possibly the $2v_x-2v_z=0$ resonance), thereby destabilizing the beam. Depending on the amount of the tune shift the third and sixth order resonances may have to be examined (at operating tunes of approximately $v_x=4.01$ and $v_z=4.11$).

QUICK REFERENCE
AGS BOOSTER PARAMETER LIST

	Protons	Polarized Protons	Heavy Ions
Energy			
Injection	200 MeV	200 MeV	$> 1 \text{ MeV/nucleon}$
Ejection	1.5 GeV	1.5 GeV	$p = 5.25 Q/A (\text{GeV}/c)/\text{nucleon}$
No. of Particles/Pulse	$1.5 - 3 \times 10^{13}$	$\sim 10^{12}$	$15 \times 10^9 (\text{S}), 3 \times 10^9 (\text{Au})$
Lattice		201.78 m (1/4 AGS)	
Circumference		13.75099 m	
Magnetic bend radius		6	
Periodicity		24 FODO	
Number of cells		8.4075 m	
Cell length		72.3° / 72.45°	
Phase advance/cell		4.82/4.83	
v_x/v_y (nominal)		13.6/3.7 m	
β_y max/min		2.95 m	
z_p max		4.831	
transition γ			
RF System			
Number of stations	2	2	2
Harmonic number	3	3	3
Frequency range (MHz)	2.5 — 4.11	2.5 — 4.11	0.200 — 2.5
Peak RF voltage	90	90	17
Acceleration time (ms)	62	62	500
Repetition rate	7.5 Hz (4/AGS pulse)	1 Hz (1/AGS)	1 Hz (1/AGS)
Dipoles			
Number		36	
Length (magnetic)		2.4 m	
Gap		82.55 mm	
Vacuum chamber aperture		66 mm	
Good field region ($< 10^{-4}$)		16 × 6.6 cm	
Injection field (kG)	1.56	1.56	0.108 A/Q
Ejection field	5.46	5.46	12.74
Quadrupoles			
Number		48	
Length (magnetic)		50.375 cm	
Aperture		16.5 cm	
Vacuum chamber aperture		15.25 cm	
Injection pole tip field (kG)	1.02	1.02	0.068 A/Q
Ejection pole tip field (kG)	3.6	3.6	8.3
Field Quality 6/2		0.0	
All other harmonics		$< 10^{-4}$	
Chromaticity Sextupoles			
Number		2 × 12	
Length (magnetic)		10 cm	
Max. pole tip field (kG)		3.0	
Max. Vacuum Pressure		$3 \times 10^{-11} \text{ torr}$	

Reference: Z. Parsa, Booster Parameter List, BNL-39311, 1987;
and Design Manual.

TABLE 1. Isotopes, Charge States, and Ionic Masses.

	<i>Q</i>	<i>Z</i>	<i>A</i>	Ionic Rest Mass (u)	Ionic Rest Mass Energy (GeV/nucleon)
p	+1	1	1	1.00723	0.93828
d	+1	1	2	2.01355	0.93781
C	+6	6	12	11.99671	0.93125
S	+14	16	32	31.96439	0.93047
Cu	+21	29	63	62.91808	0.93029
I	+29	53	127	125.88857	0.93068
Au	+33	79	197	196.94846	0.93125

TABLE 2. Injection Energies and Fields

	<i>v/c</i>	<i>f</i> (MHz)	<i>p</i> (GeV/c)	<i>E_{inj}</i>		<i>B_{inj}</i> (kG)
				(MeV)	(MeV/nucleon)	
p	0.56662	2.5235	0.6444	200.0	200.000	1.563
d	0.1767	0.7878	0.3368	30.0	15.000	0.817
C	0.1262	0.5623	1.4211	90.0	7.500	0.575
S	0.1000	0.4457	2.9925	150.0	4.688	0.519
Cu	0.0782	0.3485	4.5969	180.0	2.857	0.531
I	0.0595	0.2653	7.0489	210.0	1.554	0.590
Au	0.0473	0.2131	8.7805	210.0	1.066	0.545

TABLE 3. Ejection Energies and Fields — $B_{\max} = 12.74$ kG

	<i>v/c</i>	<i>f</i> (MHz)	<i>p</i> (GeV/c)	<i>E_{eject}</i>		<i>B_{eject}</i> (kG)
				(GeV)	(GeV/nucleon)	
p	0.9230	4.114	2.251	1.500	1.5000	5.453
d	0.8699	3.877	3.308	1.927	0.9635	8.024
C	0.8714	3.884	19.847	11.602	0.9668	8.024
S	0.8716	3.885	52.926	30.952	0.9672	9.170
Cu	0.8534	3.804	95.932	53.810	0.8541	11.081
I	0.7000	3.522	152.345	74.623	0.5880	12.743
Au	0.6863	3.061	173.353	68.050	0.3500	12.743

Reference: Z. Parsa, Booster Parameter List, BNL-39311, 1987;
and Design Manual.

TABLE 1. Isotopes, Charge States, and Ionic Masses.

12

	<i>Q</i>	<i>Z</i>	<i>A</i>	Ionic Rest Mass (u)	Ionic Rest Mass Energy (GeV/nucleon)
p	+1	1	1	1.00728	0.93828
d	+1	1	2	2.01355	0.93781
C	+6	6	12	11.99671	0.93125
S	+14	16	32	31.96439	0.93047
Cu	+21	29	63	62.91808	0.93029
I	+29	53	127	126.88857	0.93068
Au	+63	79	197	196.94846	0.93126

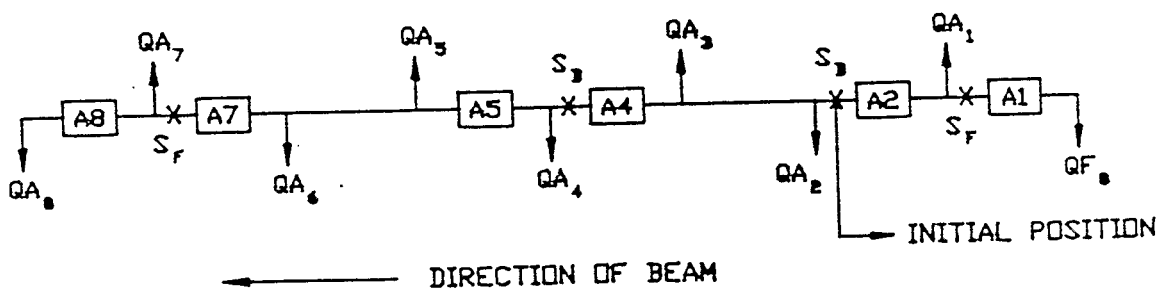
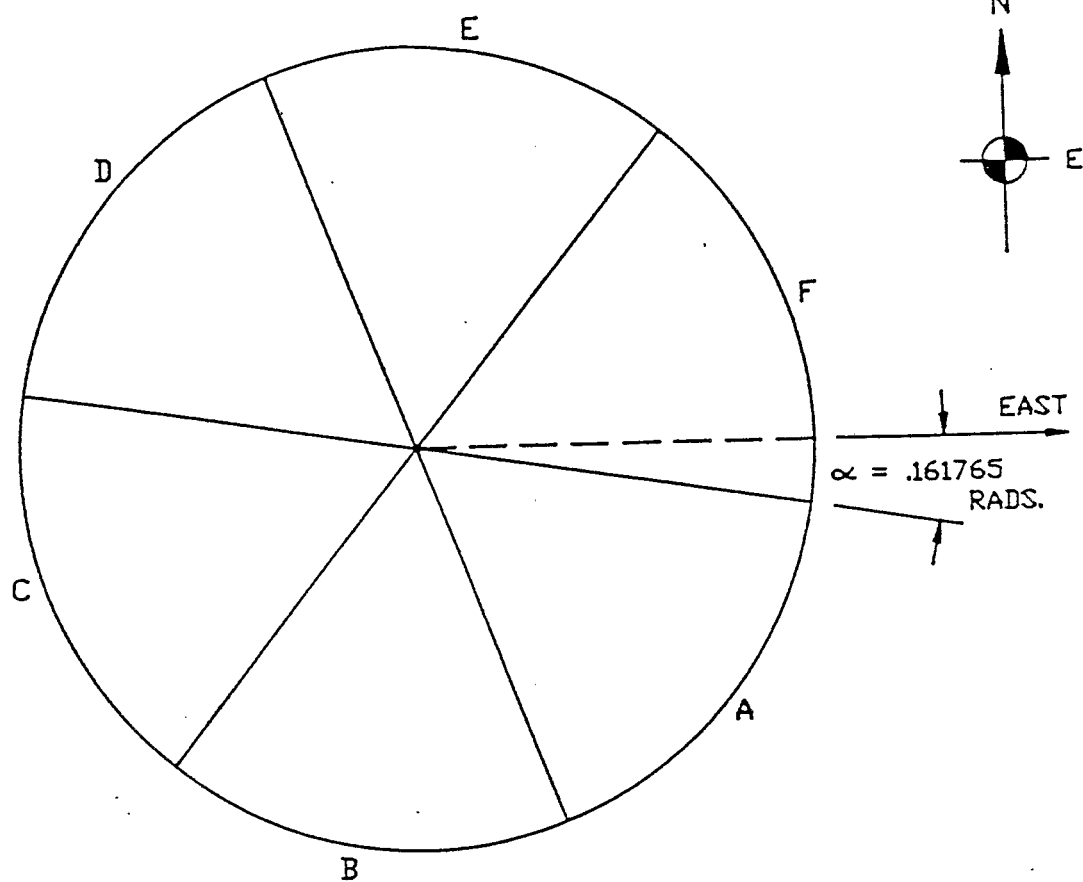
TABLE 2. Injection Energies and Fields

	<i>v/c</i>	<i>f</i>	<i>p</i>	<i>E_{inj}</i>		<i>B_{inj}</i>
				(MHz)	(GeV/c)	
p	0.5662	2.5235	0.6444	200.0	200.000	1.563
d	0.1767	0.7873	0.3368	30.0	15.000	0.817
C	0.1262	0.5623	1.4211	90.0	7.500	0.575
S	0.1000	0.4457	2.9925	150.0	4.688	0.519
Cu	0.0782	0.3485	4.5969	180.0	2.857	0.531
I	0.0595	0.2653	7.0489	210.0	1.654	0.540
Au	0.0418	0.2131	8.7805	210.0	1.066	0.645

TABLE 3. Ejection Energies and Fields — $B_{\max} = 12.74$ kG

	<i>v/c</i>	<i>f</i>	<i>p</i>	<i>E_{eject}</i>		<i>B_{eject}</i>
				(MHz)	(GeV/c)	
p	0.9230	4.114	2.251	1.500	1.5000	3.459
d	0.8699	3.877	3.308	1.927	0.9635	8.024
C	0.8714	3.884	19.847	11.602	0.9668	8.024
S	0.8716	3.885	52.926	30.952	0.9672	9.110
Cu	0.8534	3.804	95.932	58.810	0.8541	11.081
I	0.7000	3.522	152.345	74.628	0.5880	12.743
Au	0.6863	3.061	173.358	68.050	0.3500	12.743

Reference: Z. Parsa, Booster Parameter List, BNL-39311, 1987;
and Design Manual.



↑ = FOCUSING QUADRUPOLE □ = BENDING MAGNET (DIPOLE)
 ↓ = DEFOCUSING QUADRUPOLE X = SEXTUPOLE

FIG. 2 a) Schematic Diagram of the Booster and
b) Components of the Superperiod

including two families of chromaticity correcting sextupoles (chosen), located at 1.7 (SF), 2.4 (SD) per superperiod (each of 10 cm length with aperture of 16.52 cm).

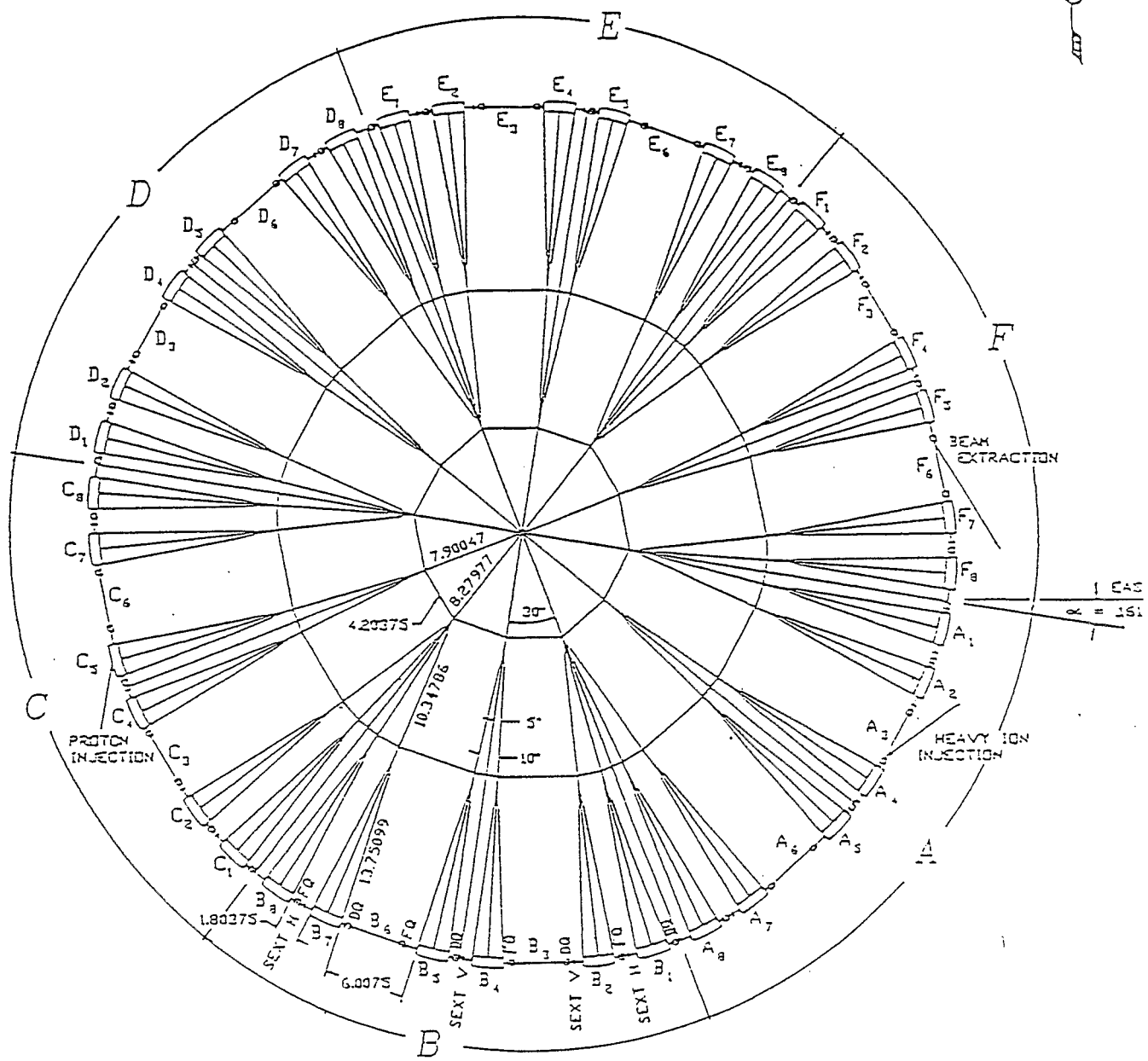
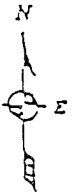


Figure 3. The layout of the Booster.

0 5
METERS

NOTE: ALL DIMENSIONS ARE IN METERS

Reference: Z. Parsa, Booster Parameter List, BNL-39311, 1987;
and Design Manual.

TABLE 4 RF Systems.

15

	P	π	S^{-14}	Au^{-22}
RF Amplitude				
Injection	90 kV	7.35 kV	0.51 kV	1.5 kV
Ejection	90 kV	40 kV	17 kV	17 kV
Harmonic Number	3	3	3	3
RF Frequency				
Injection	2.5 MHz	2.5 MHz	0.445 MHz	0.205 MHz
E/A	200 MeV	200 MeV	4.69 MeV	1.07 MeV
Ejection	4.11 MHz	4.11 MHz	4.13 MHz	3.06 MHz
Phase Space Area/A	$\geq 1.0 \text{ eV-s}$	0.3 eV-s	0.066 eV-s	0.056 eV-s
Intensity (particles (per bunch))	10^{13}	$\sim 1 \times 10^{11}$	5×10^9	8×10^9
Total Gap Impedance ($f_{rf} = 4.1 \text{ MHz}$)	< 24 kΩ	No limit	No limit	No limit
Acceleration Time	62 ms	$\leq 0.5 \text{ s}$	$\leq 0.5 \text{ s}$	$\leq 0.5 \text{ s}$
Maximum Power Delivered to Beam	150 kW	< 2 kW	< 1.0 kW	< 2 kW
Maximum \dot{B} \dot{B}_{ini}	9.5 T/s 1.5 T/s	4.5 T/s ?	4.5 T/s < 0.15 T/s	4.5 T/s < 0.15 T/s

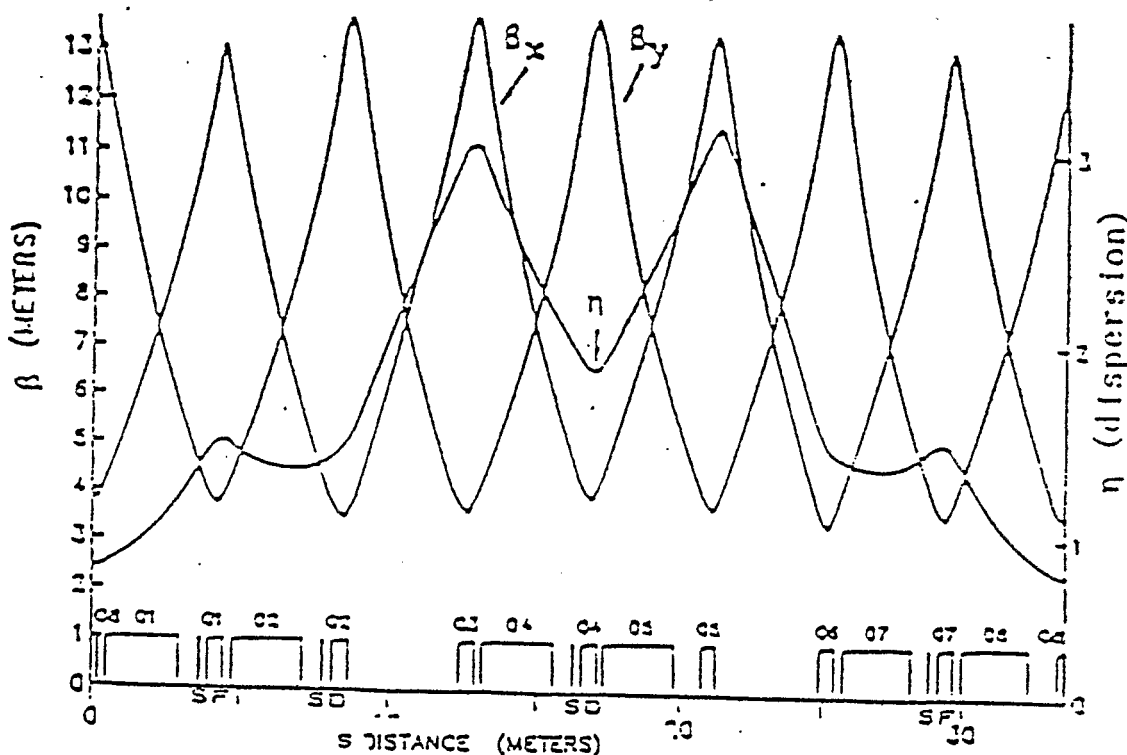


Fig. 4, shows the betatron functions and the amplitude dependence of tunes for the AGS Booster.

We have studied the effect of the systematic resonances in the Booster; and in Table II and III, we present some of our results (obtained using program HARMON and NONLIN), for the third and fourth order resonances. These and higher order resonances are discussed in Reference [2], since HARMON is limited to the calculation of fourth order resonances.

Table I., shows the perturbation to tune (Q'_x , Q'_z) at the corresponding operating (linear) tunes (Q_x , Q_z) at which the resonances were investigated.

TABLE I. : Tune Shift

Operating Tunes		Perturbed Tunes	
<u>Q_x</u>	<u>Q_z</u>	<u>Q'_x</u>	<u>Q'_z</u>
4.82	4.83	4.820476	4.834616
4.501	4.511	4.500944	4.514804
4.001	4.011	3.982678	4.000854

Tables I - III shows that the results obtained from HARMON and NONLIN agrees quite well with the largest difference in the fourth order resonances (due to the 2nd order sextupole effects).

TABLE II AGS-Booster Lattice [NONLIN]

<u>Resonances</u>		<u>Strength</u>	<u>Stop Bandwidth</u>	<u>Tunes</u>	
				<u>v_x</u>	<u>v_z</u>
3v _x	=12	6.0420E-08	0.010876	4.001	4.011
3v _x	=18	2.1010E-07	0.037819	4.001	4.011
v _x +2v _z	=12	3.5657E-07	0.035657	4.001	4.011
	=18	1.0916E-06	0.10916	4.001	4.011
-v _x +2v _z =0		2.6354E-07	0.015813	4.001	4.011
	=6	1.7728E-06	0.10637	4.001	4.011
4v _x	=18	9.5171E-07	0.003046	4.501	4.511
4v _z	=18	2.2488E-08	0.007196	4.501	4.511
2v _x +2v _z =18		3.0213E-08	0.004834	4.501	4.511
2v _x -2v _z =0		3.9000E-07	0.031200	4.001	4.011
		1.5020E-07	0.021016	4.501	4.511
		1.6589E-07	0.013271	4.820	4.83
4v _x	=24	1.8992E-07	0.006077	4.820	4.83
4v _z	=24	6.5537E-08	0.020972	4.820	4.83
2v _x +2v _z =24		6.8447E-08	0.010952	4.820	4.83
2v _x -2v _z =-6		5.2447E-08	0.0041957	4.820	4.83
4v _x +2v _z =18		1.2538E-06	0.5010	4.001	4.011
	=24	2.4479E-07	0.097916	4.001	4.011
6v _x	=18	7.4445E-07	0.53600	4.001	4.011
	=24	1.1435E-07	0.08233	4.001	4.011

TABLE III AGS-Booster Lattice [HARMON]

<u>Resonances</u>		<u>Strength</u>	<u>Stop Bandwith</u>	<u>Tunes</u>	
				<u>v_x</u>	<u>v_z</u>
3v _x	=12	6.04187E-08	0.010876	4.001	4.011
3v _x	=18	2.10103E-07	0.037819	4.001	4.011
v _x +2v _z	=12	3.56559E-07	0.035657	4.001	4.011
	=18	1.09163E-06	0.10916	4.001	4.011
-v _x +2v _z	= 0	1.633876E-07	*****	4.001	4.011
	= 6	1.77282E-06	*****	4.001	4.011
4v _x	=18	7.64062E-09	0.001223	4.501	4.511
4v _z	=18	1.08154E-08	0.001731	4.501	4.511
2v _x +2v _z	=18	3.13890E-08	0.002511	4.501	4.511
2v _x -2v _z	= 0	1.9042E-07	*****	4.001	4.011
		1.10073E-07	*****	4.501	4.511
		1.2424E-07	*****	4.820	4.830
4v _x	=24	6.8891E-09	0.0011023	4.820	4.830
4v _z	=24	1.84457E-08	0.00295135	4.820	4.830
2v _x +2v _z	=24	7.002513E-08	0.005602	4.820	4.830
2v _x -2v _z	=-6	13.446	*****	4.820	4.830

Figure 5 shows the variation of the betatron ($\Delta\beta/\beta$) and dispersion ($\Delta\eta/\eta$) functions (at operating tune of 4.82) due to space charge tune shift, resonances (peaks) appears at tunes of 4 and 4.5 respectively.

η = Dispersion
 β = Betatron funct.
 $co \equiv$ Closed orbit

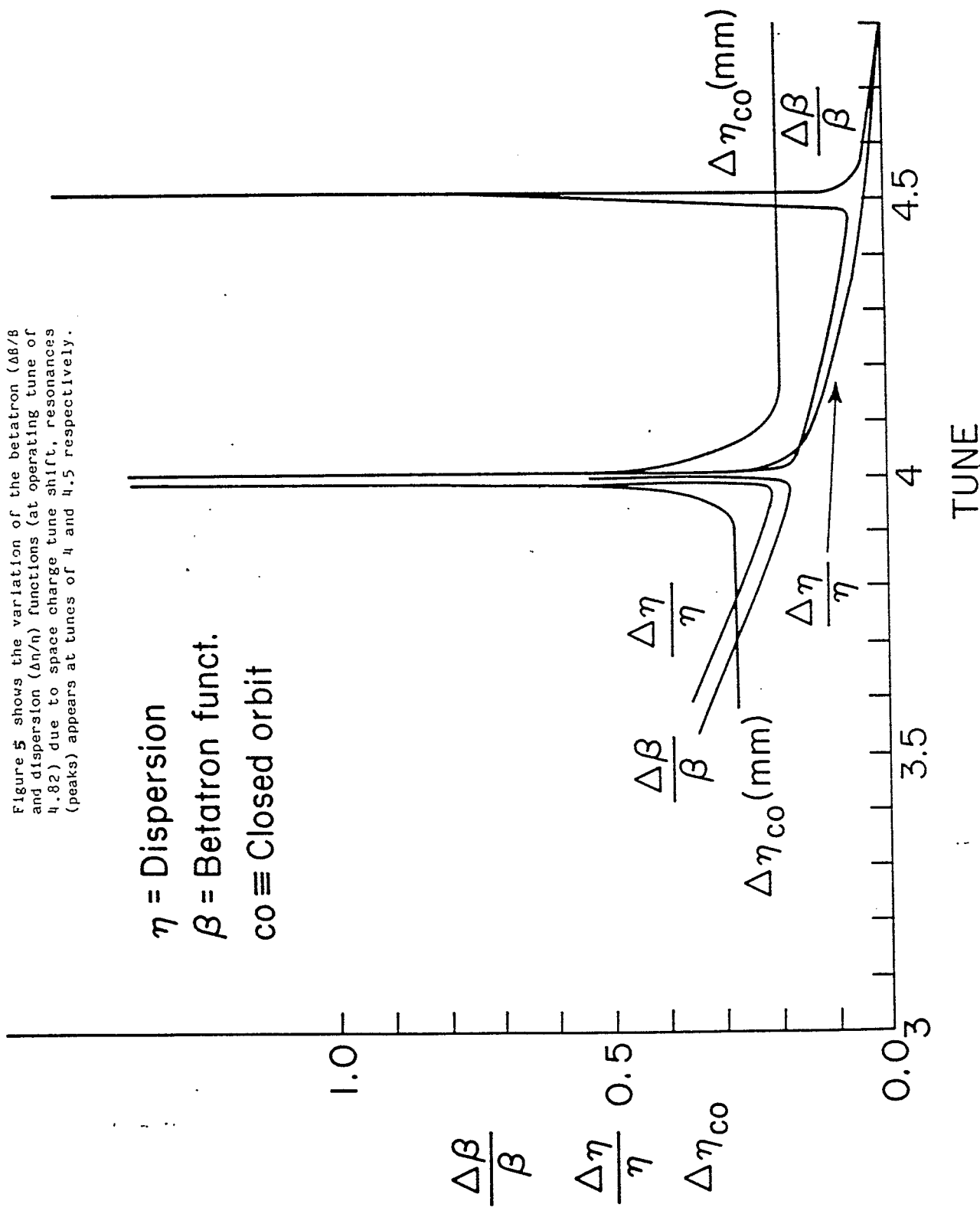


FIGURE 5

Figure 5
Variation of the betatron function (showing structure
of the resonance) at operating tune of about 4.5.

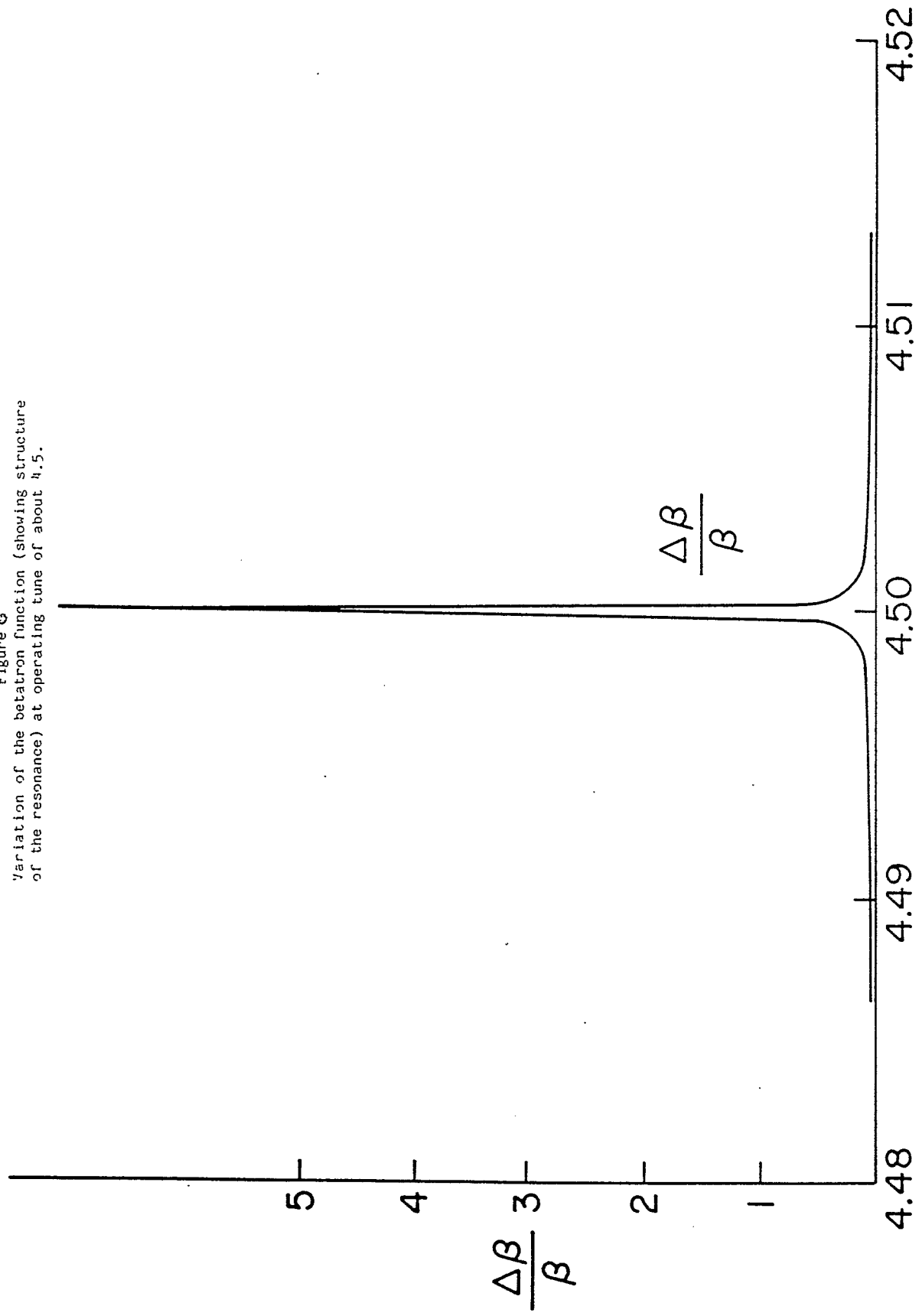
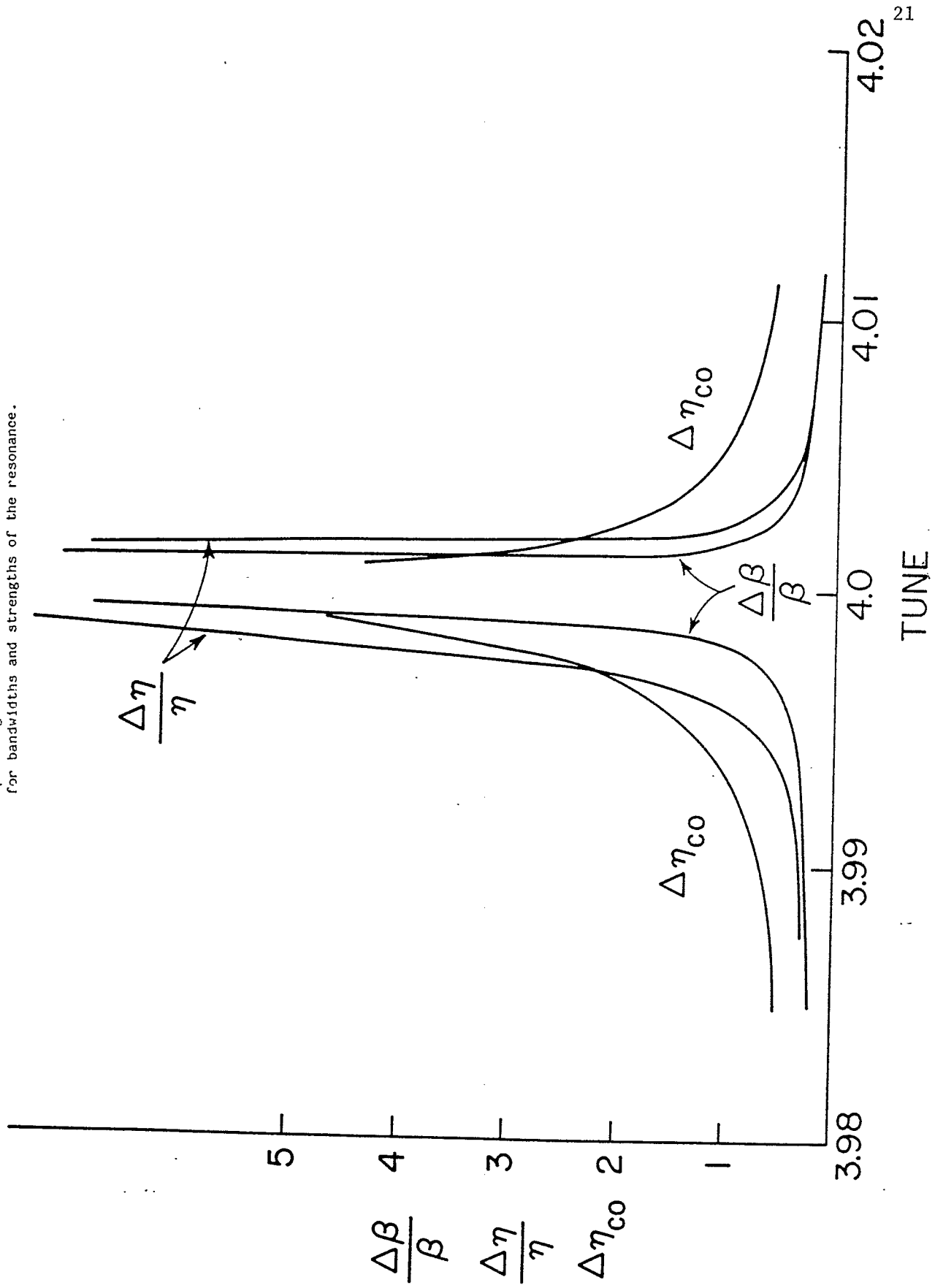


FIGURE 6

Figure 21

Variation of the betatron and dispersion function (at operating tune of about 4.0). See Tables I and/or II for bandwidths and strengths of the resonances.



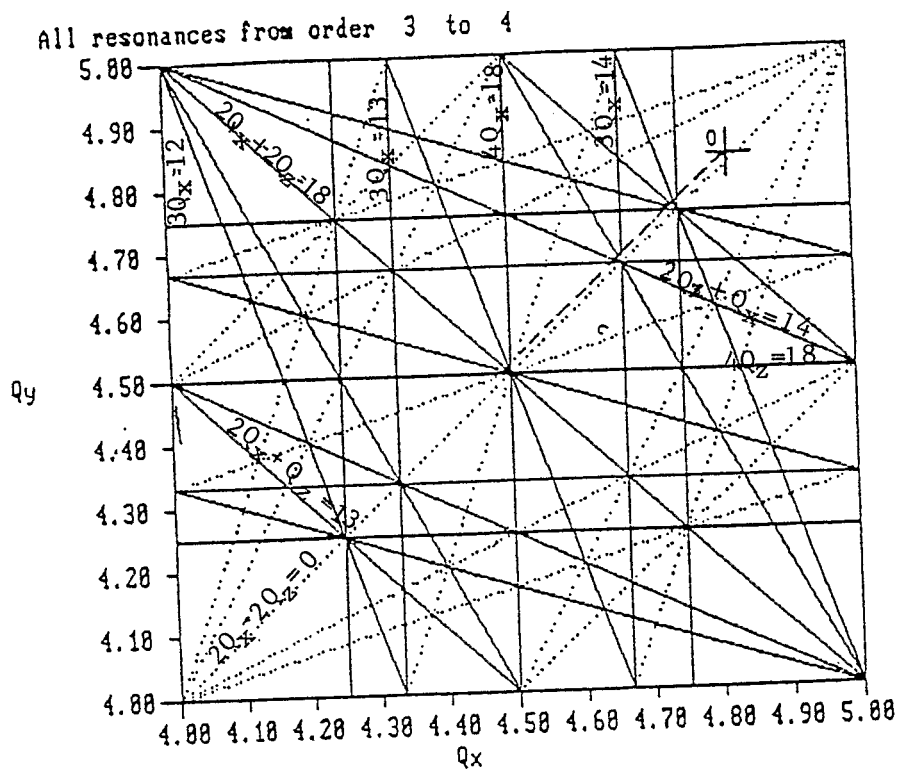


Figure 8 shows the tune diagram and resonance lines for the Booster with operating point $O(4.82, 4.83)$. The dashed line shows the expected region of tune shift due to the space charge.

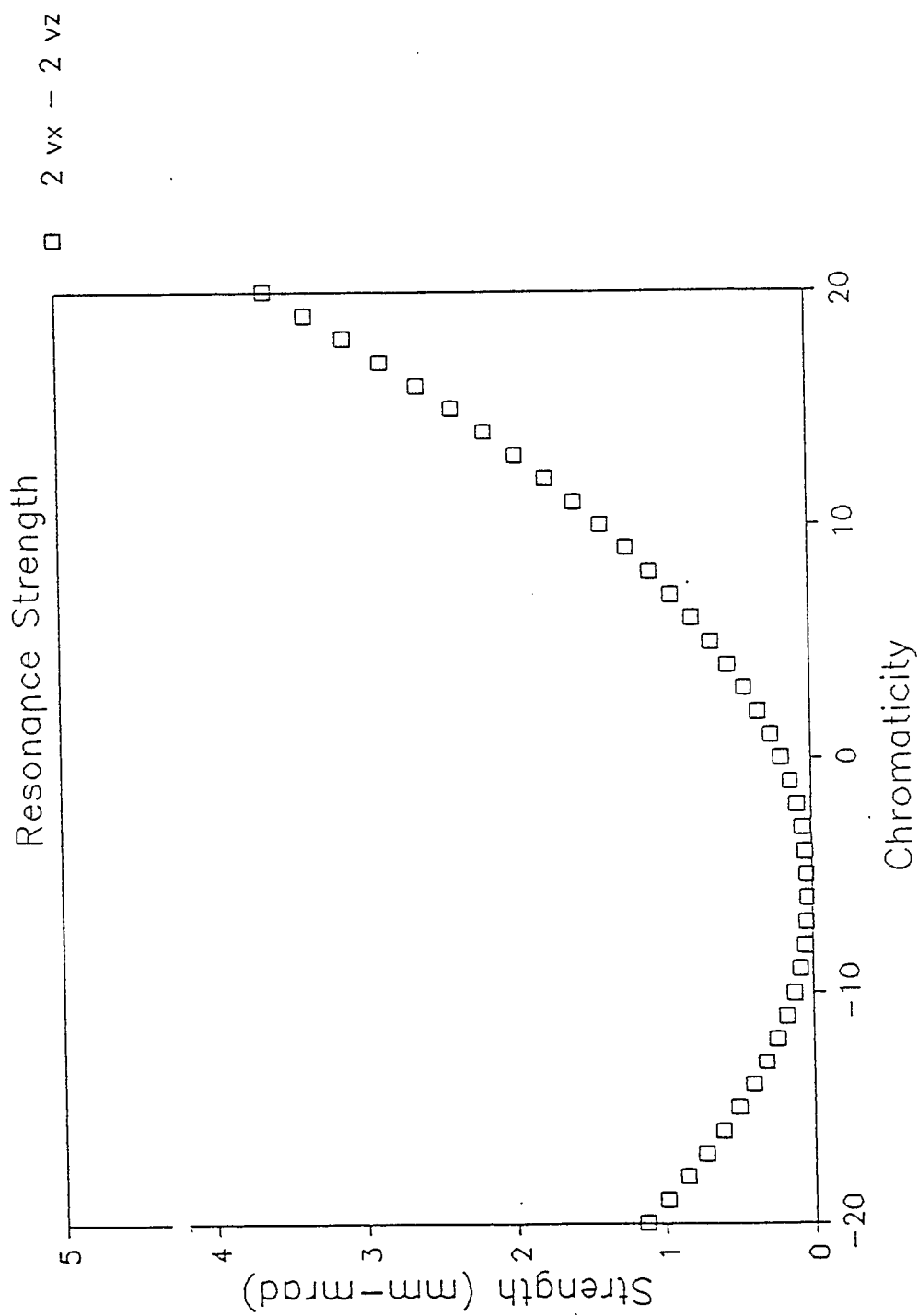
Table IV includes the Bandwidth with perturbed tunes as well as the maximum total value of the emittance; Generating Function Resonance strengths; Hamiltonian Resonance strengths; Stop Bandwidth; Fixed Points; Island Width and Chirikov criteria for the Booster.

TABLE IV

Chrom	Bandwidth	Max Et /pi	Gen. Fun.		Hamiltonian	
			Res.	Str.	Res.	Str.
-6. 0000000	2Vx-2Vz	108. 9210000	.0370876		.0215430	
-6. 0156880					.0212390	
-5. 5000000	- .0172100	108. 2140000	.0370590		.0221530	
-5. 0000000	- .0186480	108. 1590000	.0383276		.0762360	
-2. 0000000	- .0254620	111. 8600000	.0984171			
0	- .0282800	118. 8650000	.1999800		.1658900	
Island Width and Chirikov Criterion						
Stop	Fixed Points					
Chrom	Bandwidth					
-6. 0000000	.0017235	.0010516	6. 5580000		.0004030	
-5. 5000000	.0016991	.0010728	8. 0864000		.0003271	
-5. 0000000	.0017723	.0010686	10. 4350000		.0002644	
-2. 0000000	.0060989	.0004842	15. 4580000		.0006143	
0	.0132710	.0003068	11. 7630000		.0017565	

Since the $2vx - 2vz$, $vx - 2vz$ and vx resonance contributions are of interest

AGS - BOOSTER with EDDY CURRENTS



in Fig. 9 we show the strength of these resonances (Generating Function Resonance strengths) as functions of the chromaticity of the Booster with eddy currents and chromaticity sextupoles.

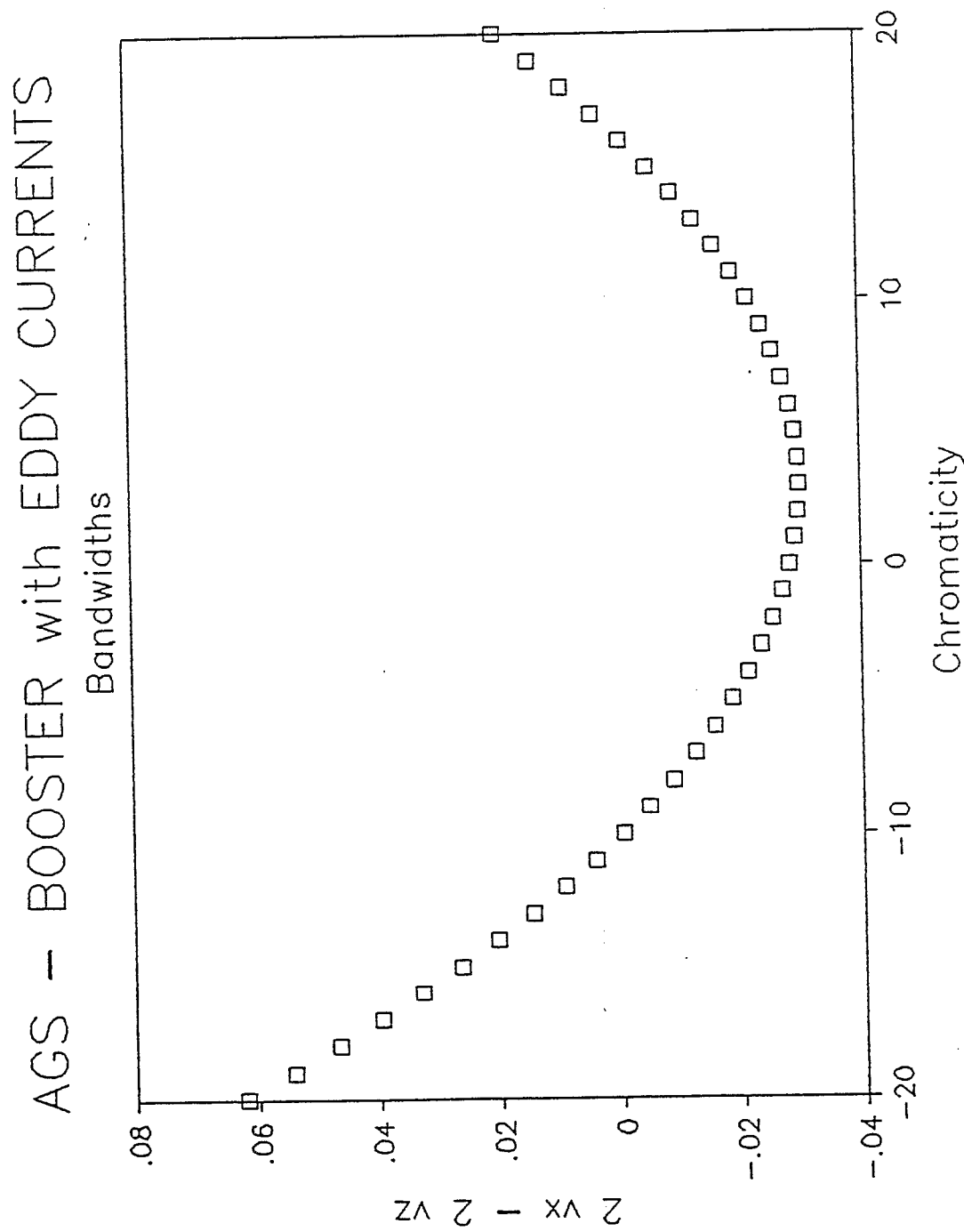


Fig. 10 shows the plot of Bandwidths versus the machine chromaticity for the $2\omega_x - 2\omega_z$ resonance (for the Booster lattice with eddy currents and chromaticity sextupoles).

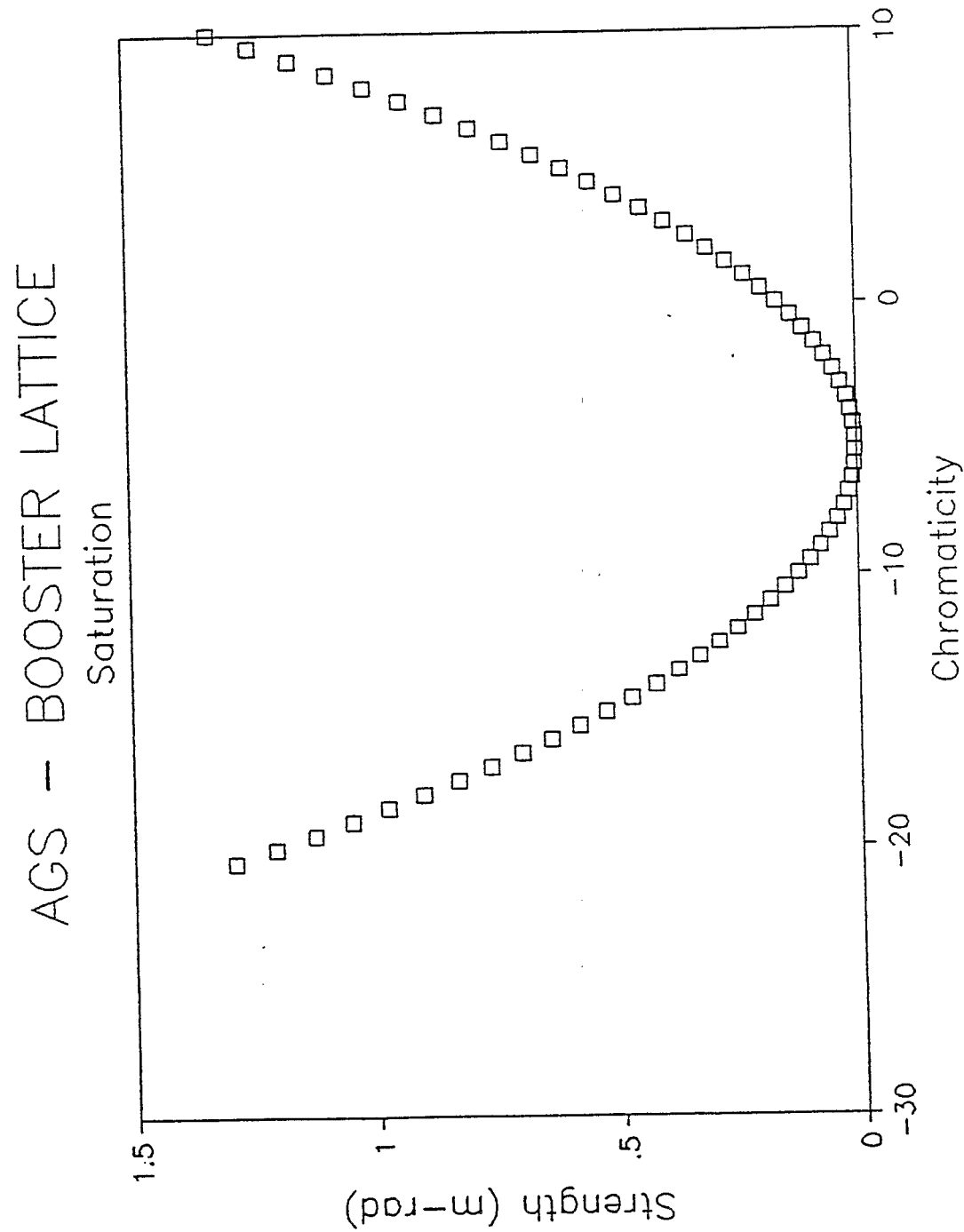


Fig. 11 shows the $2\pi x - 2\pi z$ resonance strength versus the machine chromaticity (for the Booster lattice with Saturation and chromaticity sextupoles).

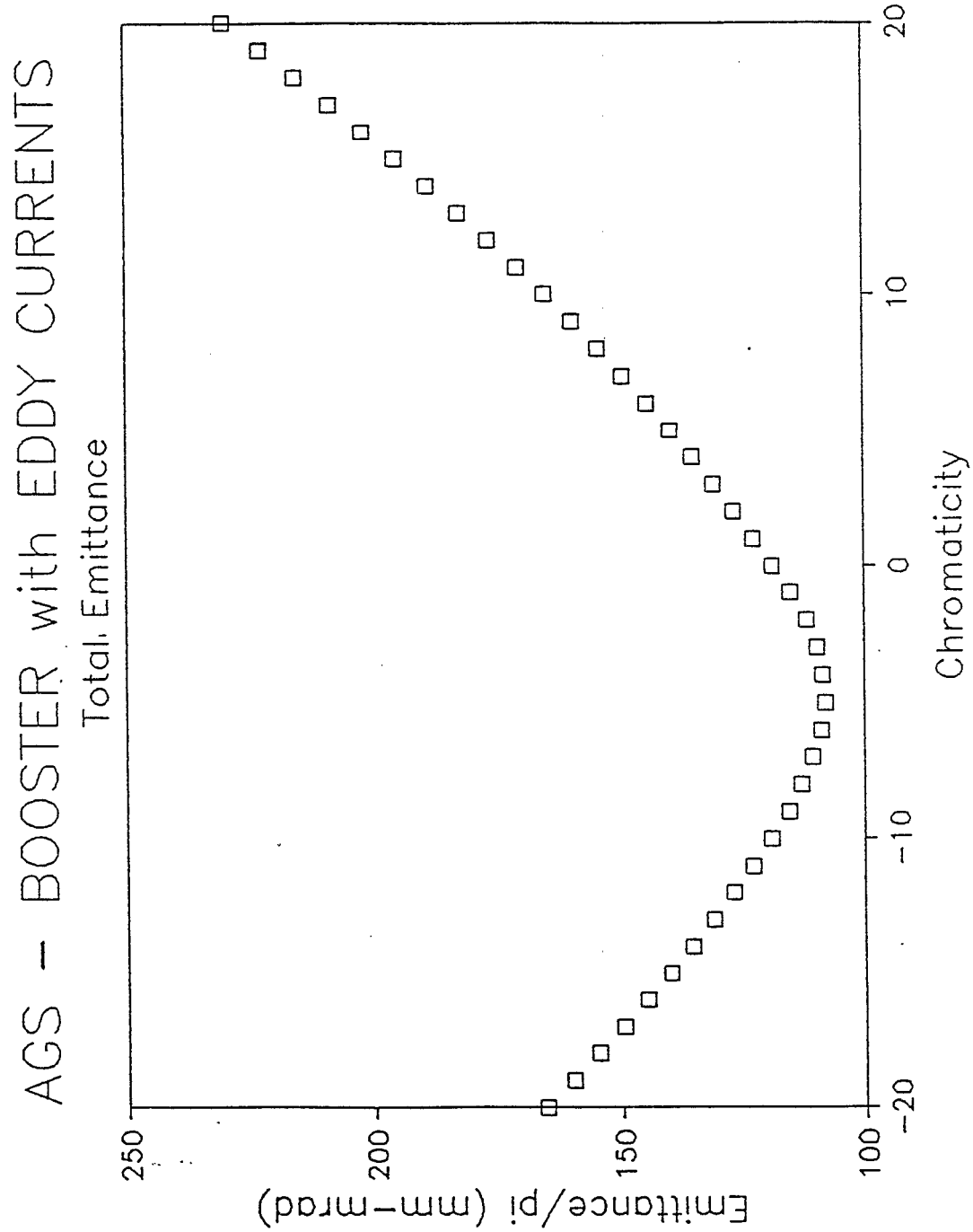


Fig. 12 shows maximum total emittance (for the Booster lattice with eddy currents and chromaticity sextupoles) versus the machine chromaticity, which agrees quite well with the results obtained from tracking.

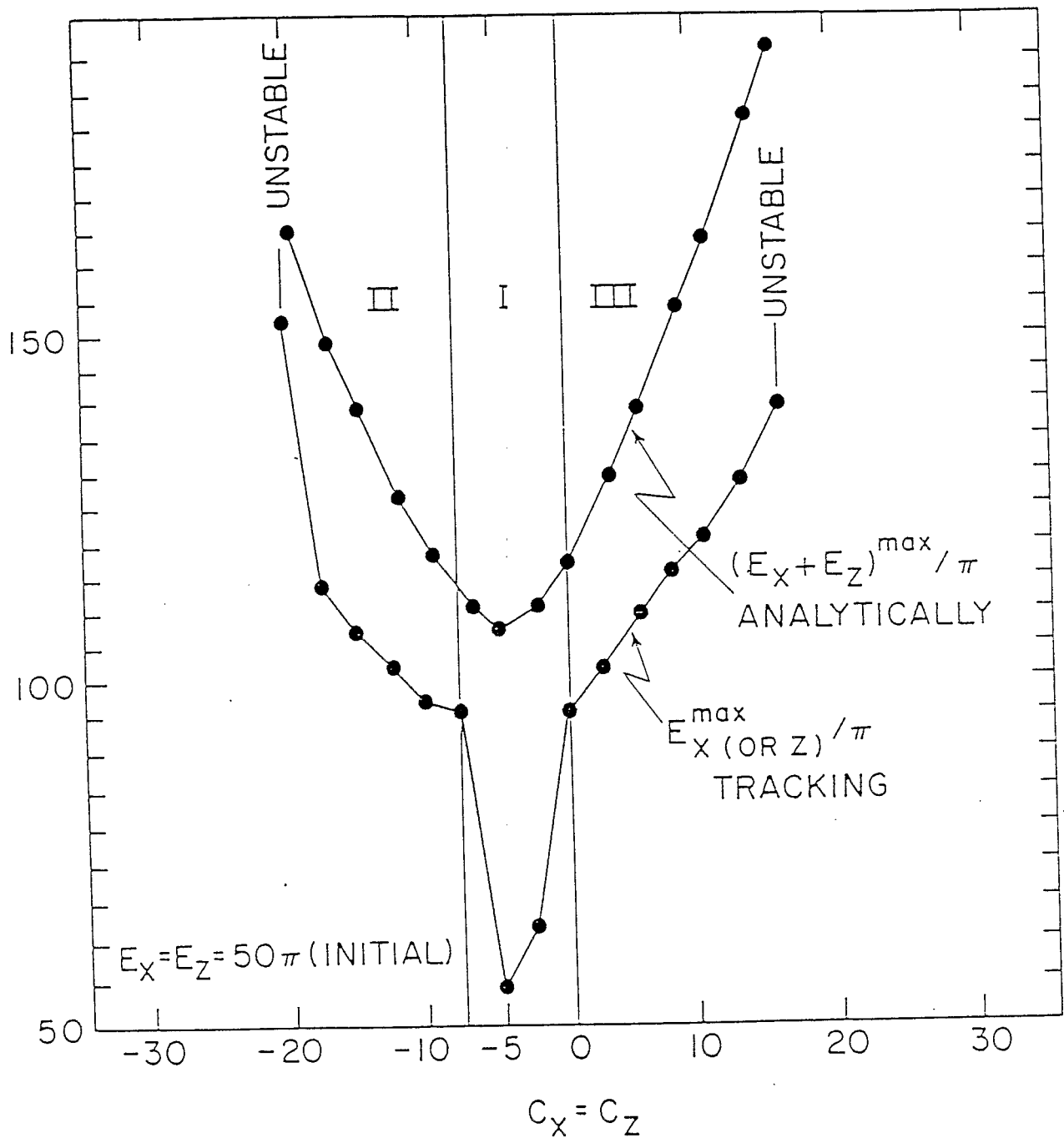


Fig. 13 shows the maximum emittance (in x or z direction) obtained from tracking³, and the maximum total emittance obtained analytically, as functions of the Booster chromaticity respectively. We note that one particle was used analytically and four particles were used in tracking. In region I, variation of the perturbed tunes (due to initial $\phi_X(s=0)$, $\phi_Z(s=0)$) are small and do not cross the $2\nu_X - 2\nu_Z = 0$ resonance for any particles. In region II and III, variation of the perturbed tune, (due to different initial phases $\phi_X(s=0)$ and $\phi_Z(s=0)$), becomes large, allowing the crossing of $2\nu_X - 2\nu_Z = 0$ resonance for some of the particles.

To relate our analytic result with those obtained from tracking we must relate the initial conditions. The initial conditions used for tracking are the phase ϕ_x ($s=0$) and emittance for the particle(s). However, the phase and the new actions K_x and K_z are the parameters for the initial conditions in our analytic approach. These initial conditions can be related with the following expressions:

$$E_x(s=0) = E_x(K_x, K_z, \phi_x(s=0), \phi_z(s=0))$$

$$E_z(s=0) = E_z(K_z, K_x, \phi_x(s=0), \phi_z(s=0))$$

If there is a strong coupling term(s) in those expressions (e.g. $2v_x - 2v_z$ for the Booster, then changing the initial phase ϕ_x and ϕ_z (for different particle(s) but keeping the same initial emittance (E_x, E_z) will produce a large spread in K_x and K_z which in turn results in a spread in the nonlinear tunes (for the particles) and the likelihood of a particle crossing the coupling resonance.

However, in tracking several particles are used, the particle that gives the smallest bandwidth ($2v_x - 2v_z$) will lead to the greatest emittance growth due to the coupling; so many particles will excite the coupling resonance while (at the same time) many others would not. The number of particles that excite this resonance depends on how large are the coefficients α_{xx} , α_{xz} , α_{zz} (see eq.12 & 13) as well as how large is the $(2v_x - 2v_z)$ resonance strength. Our analytic and tracking⁵ results (both) indicates at chromaticities $C_x = C_z = -5$,

both the α 's and resonance strengths are minimum. (This is the region where chromaticity correcting sextupoles is minimum.) This point is illustrated in Fig. 13, which shows the maximum emittance (in x or z direction) obtained from tracking (of particles) and the maximum total emittance obtained analytically (for one particle), as functions of the Booster chromaticity respectively. In region I, the strength of the coupling resonance is weak and α 's are small (hence variations of the perturbed tunes due to initial $\phi_x(s=0)$, $\phi_z(s=0)$ are small) thus no particle will cross the ($2v_x - 2v_z = 0$) coupling resonance as confirmed by tracking. However, in region II and III variations of the perturbed tunes (due to different initial phases $\phi_x(s=0)$ and $\phi_z(s=0)$, becomes large, (since the α 's are large) and the spread in K_x and K_z is larger than in Region I (because the coupling resonance is larger) thus allowing the crossing of the coupling resonance for some particles. This can be seen from the analytic (one particle) and tracking (of four particles) Plots in Fig. 13, where both methods predict the smallest contributions from nonlinearities at chromaticity of -5 for the Booster.

AGS - BOOSTER WITH EDDY CURRENTS

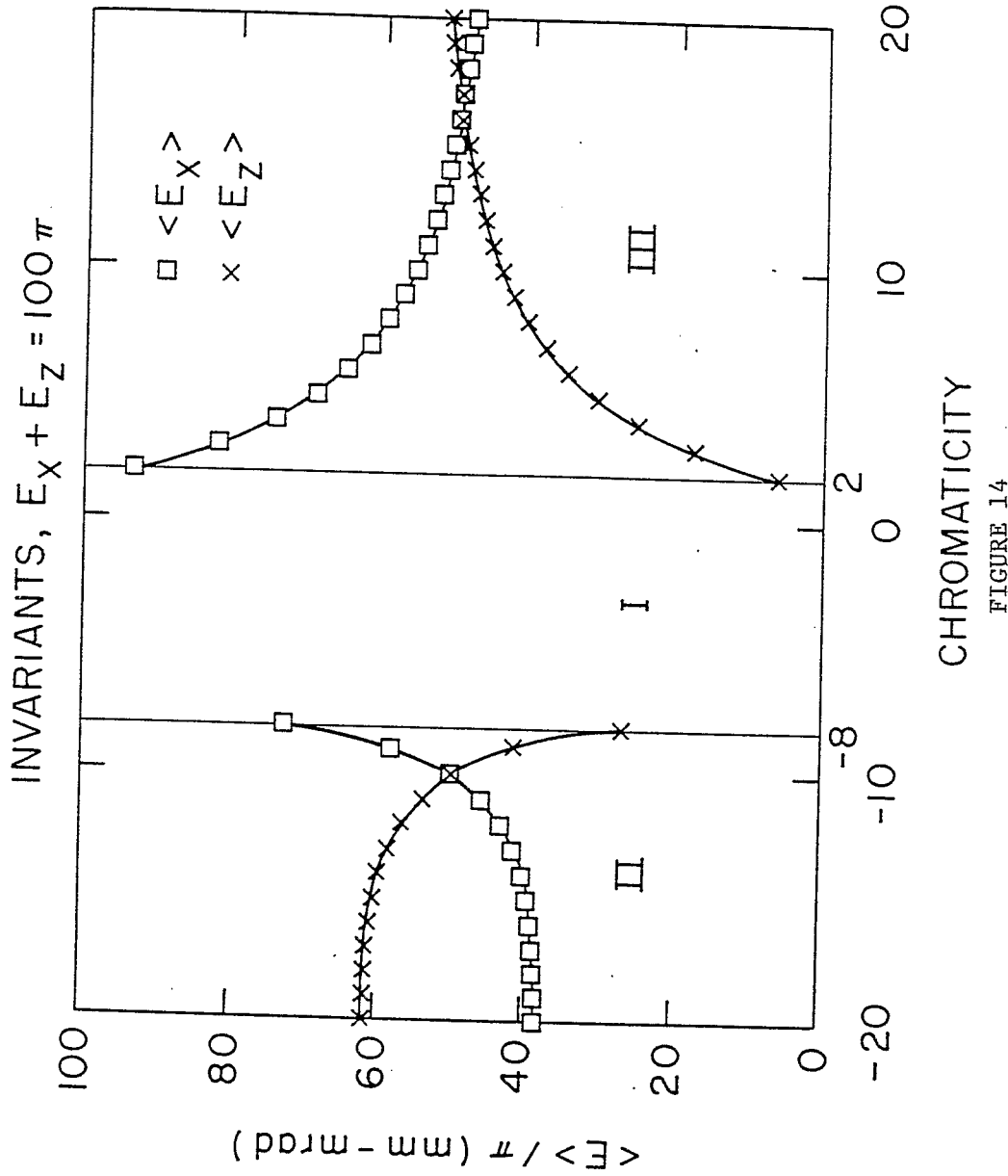


FIGURE 14

Fig. 14 shows the average emittance as a function of chromaticity of the Booster, assuming that some of the average emittance is $\leq 100\pi$ mm-mrad. In Region I, for $0 < c_x = c_z < 2$ the strength of this resonance is very strong allowing the average $\langle E_x \rangle + \langle E_z \rangle$ to be $> 100\pi$ mm-mrad, leading to a coupling as observed by tracking. However, there exist a chromaticity window between $-8 < c_x = c_z < 2$ where there is no $2v - 2v = 0$ coupling. The size of this window will increase if you decrease the total emittance which in turn decreases the total average emittance. The observed window is slightly smaller than shown in Fig. 14, because the actual sum of the averaged emittances are greater than 100 as illustrated above. This indicates that to increase the size of the window, either we decrease the total initial emittance and/or increase the number of sextupoles per superperiod.

AGS- BOOSTER WITH EDDY CURRENTS

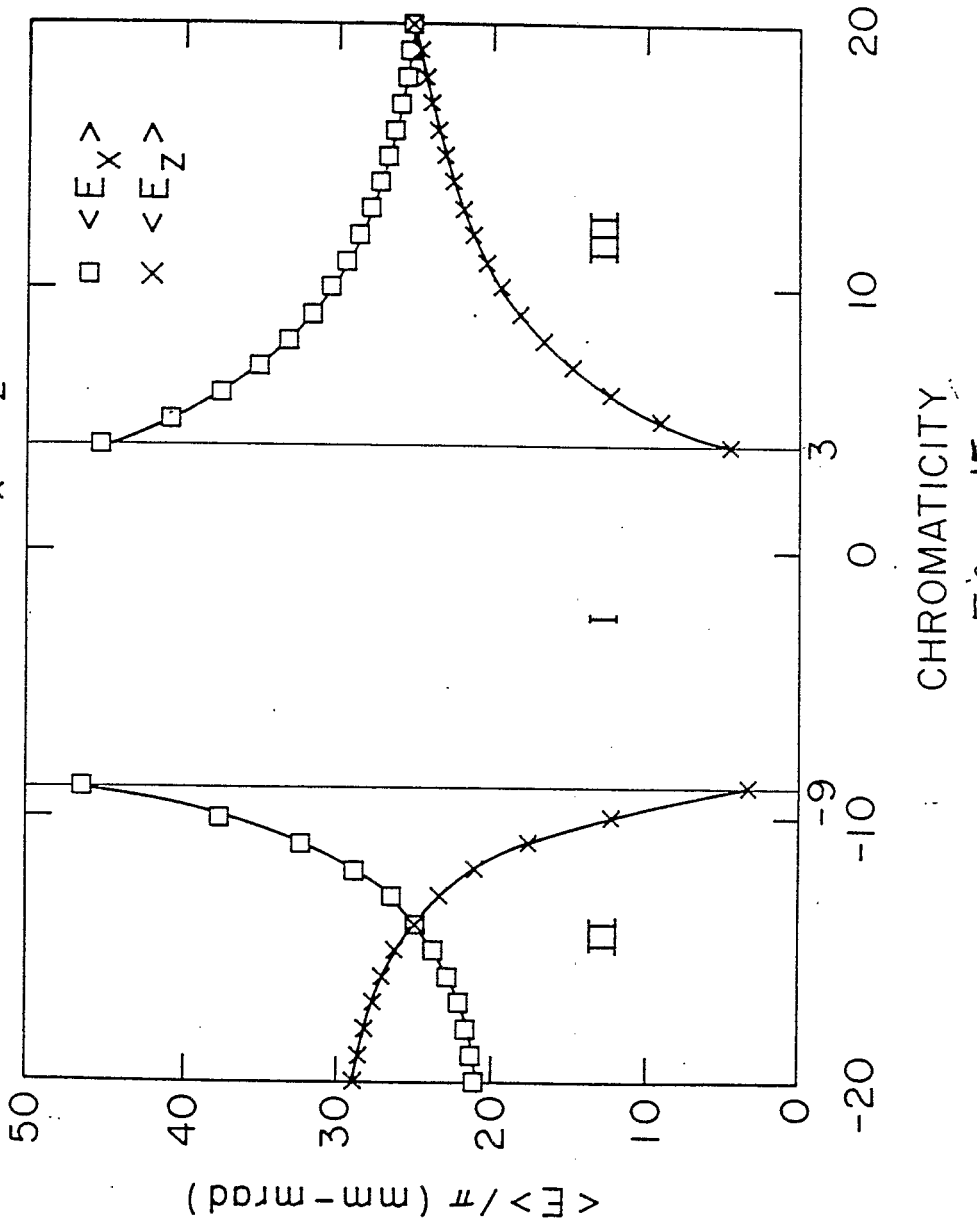
INVARIANTS, $E_x + E_z = 50\pi$ 

Figure 15

Fig. 15 illustrates the decrease in the total initial emittance from 100 to 50π mm-mrad; and the corresponding increase in the size of the chromaticity window (to $-9 < c_x = c_z < 3$).

Figure 16 shows the plot of $E_z^{1/2}$ versus $E_x^{1/2}$ (for the Booster) where the emittance values were computed with the initial conditions $\phi_x=0$, $\phi_z=0$; $K_x = E_{x_0}/2\pi$ and $K_z = E_{z_0}/2\pi$ at a given sextupole position. When the initial conditions are changed to the position of a different sextupole (multipole) the maximum values the emittance grows to remains almost the same. Thus, no preference in the choice of initial tracking position. Given ψ_x and ψ_z , using equations (9-10, 14-17) we solve for ϕ_x and ϕ_z ; then solve for E_x and E_z . The next point in the sequence is found by incrementing ϕ_x and ϕ_z by $2\pi\nu_x$ and $2\pi\nu_z$ which is the position of the same sextupole in the next revolution.

From our plots (e.g. Fig. 16) we can calculate "smear", "linear aperture" etc.

These type of plots contain the same information one would obtain from tracking program and can be used as alternative to tracking. That figure also illustrates the presence of strong coupling due to $2\nu_x - 2\nu_z = 0$ resonance which is indicated by the negative slope of the shaded area.

Similar observations have been made using tracking programs PATRICIA (F.Dell) and ORBIT (G.Parzen).

AGS - BOOSTER LATTICE
Averaged Emittance = 50π mm-mrad

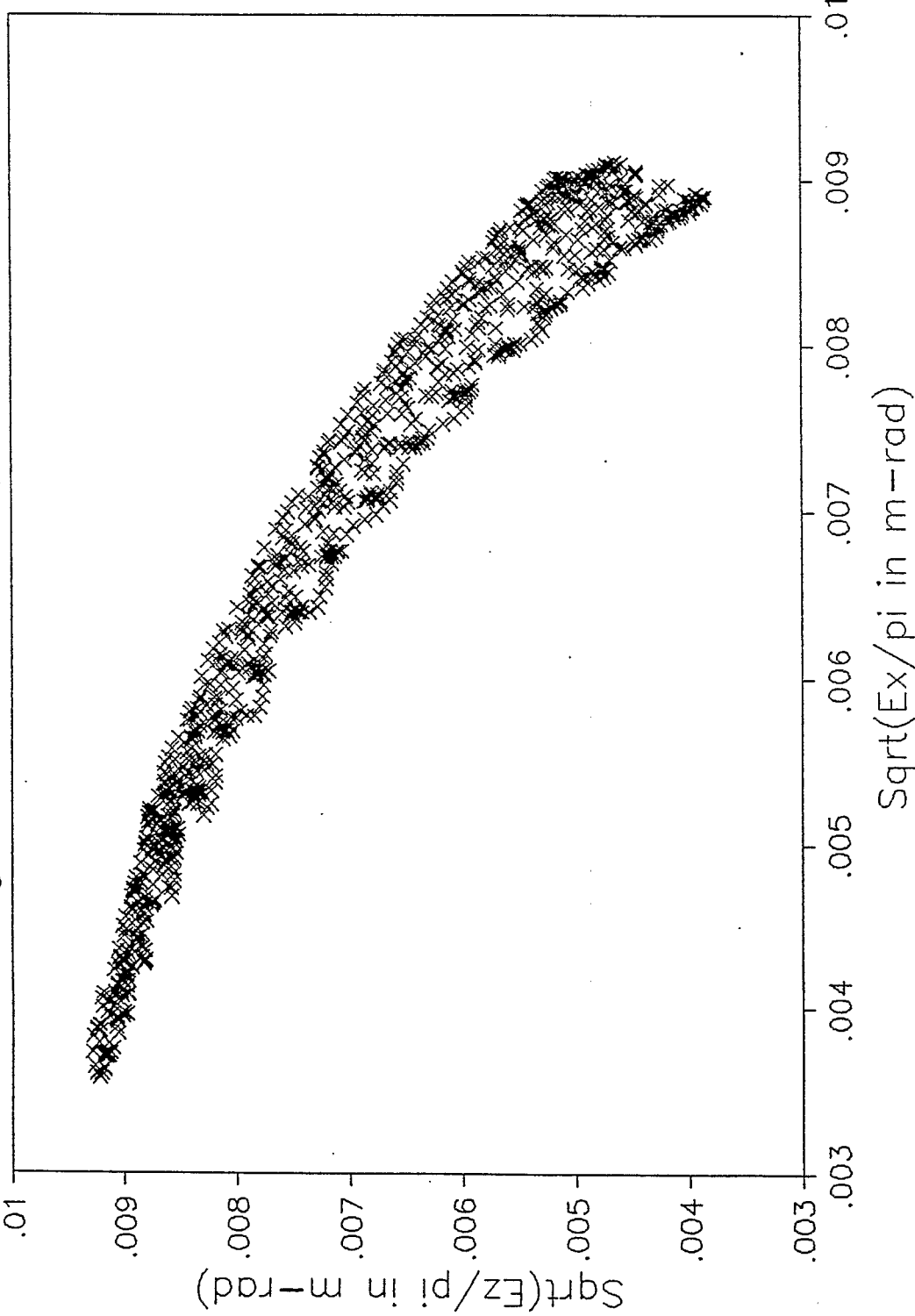


FIGURE 16

Fig. 16 shows plot of $E_z^{\frac{1}{2}}$ versus $E_x^{\frac{1}{2}}$ (for the Booster) where the emittance values were computed with the initial conditions $\phi_z = 0$, $x_0 = E_z / 2\pi$ and $K_z = E_x / 2\pi$ at a given sextupole position (see Fig. 2). If initial conditions are changed to (start the tracking at) the position of another sextupole (multipole) the maximum value of the emittance would remain about the same.

AGS - BOOSTER LATTICE

Averaged Emittance = $50\pi \text{ mm-mrad}$

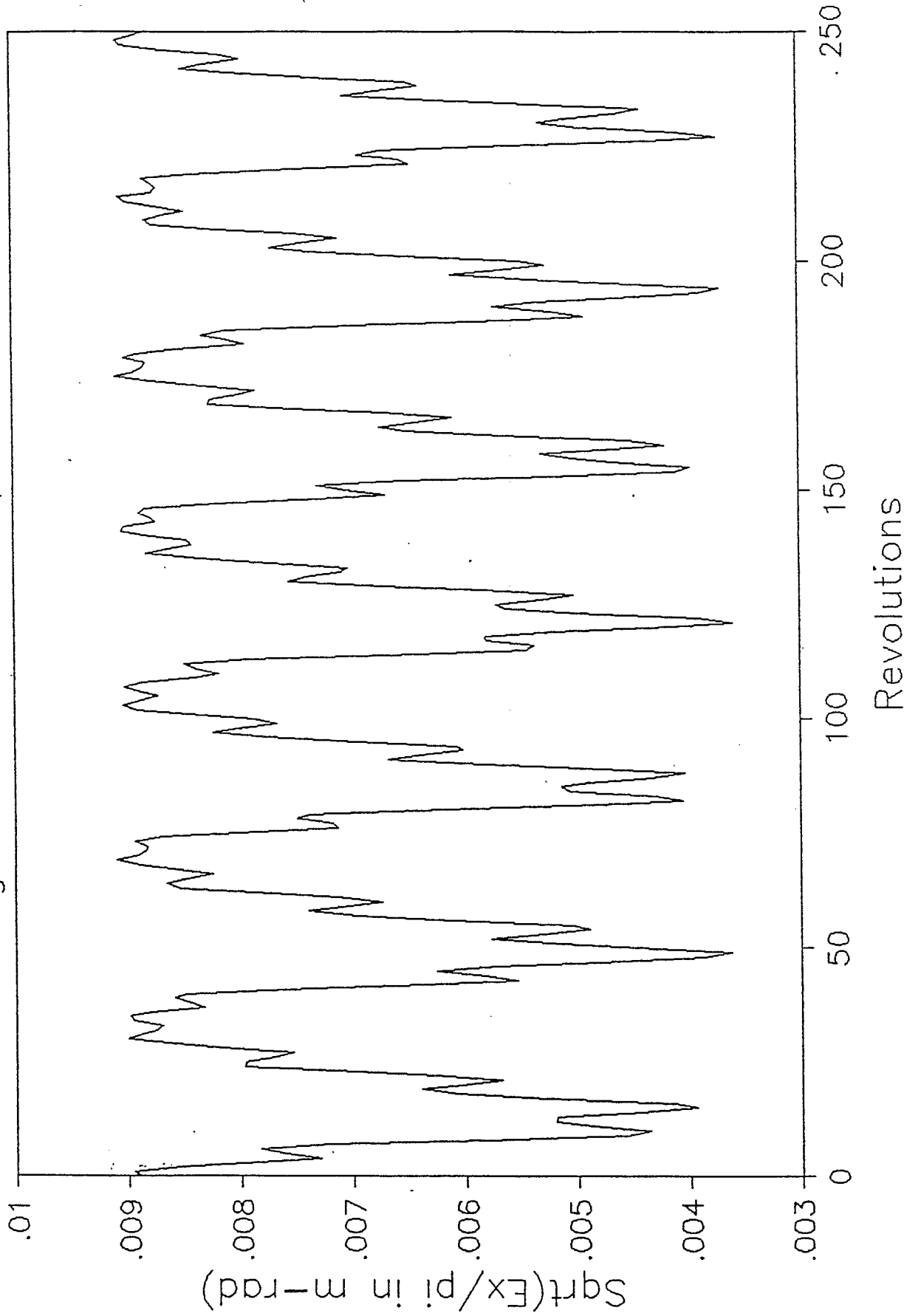


Figure 17: $\frac{\nu}{E_x^2}$ versus number of revolutions.

AGS - BOOSTER LATTICE

Averaged Emittance = $50\pi \text{ mm-mrad}$

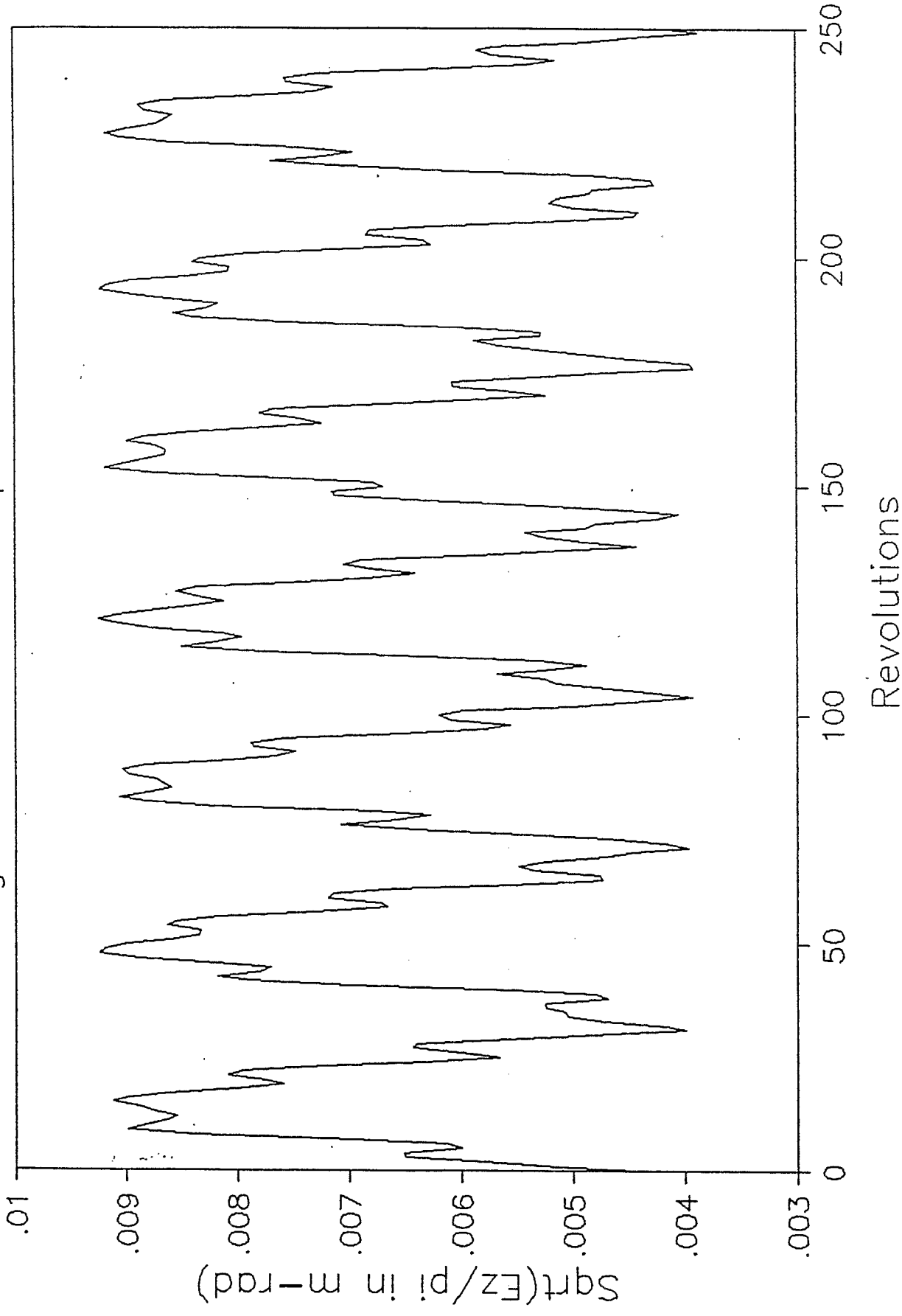


Figure 18 : $E_z^{\frac{1}{2}}$ versus number of revolutions. These two figures differ in phase due to coupling of $2\nu_x - 2\nu_z = 0$ resonance.

AGS - BOOSTER LATTICE

Averaged Emittance = $50\pi \text{ mm-mrad}$

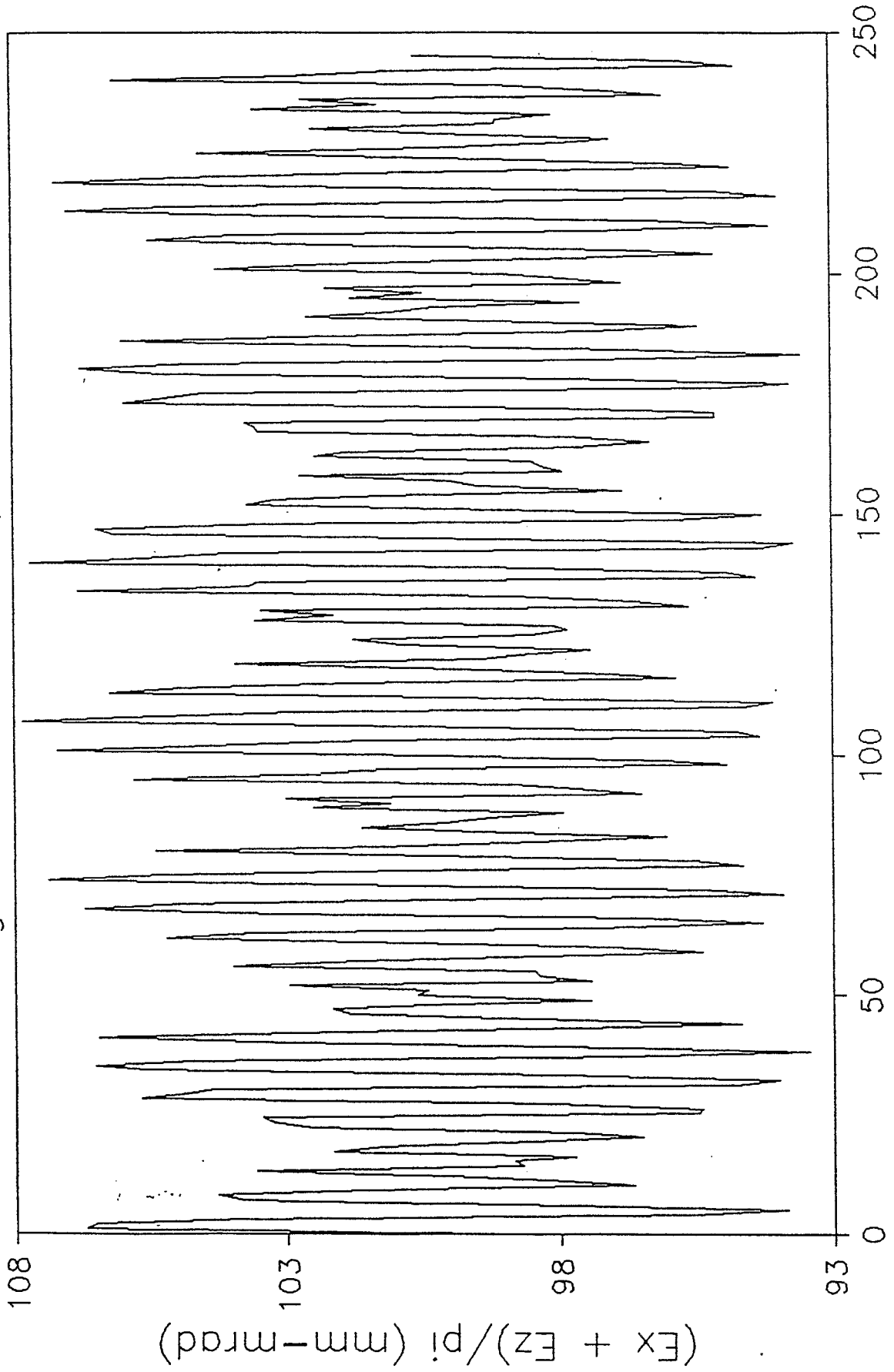


Figure 19, gives the plot of $E_x + E_z$ versus revolutions, which is the invariant of the $2\nu_x - 2\nu_z = 0$ resonance (assuming there are no other resonances). The influence and importance of other resonances is indicated by this figure.

Comparison of the phase

plots, Figures 20 and 21 obtained analytically with Figures 22 and 23 (obtained from tracking⁵) indicates good agreement (e.g. for the maximum x , \dot{x} and z , \dot{z}). However, the fine structures seen in Figures 20 and 21 are not apparent in Figures 22 and 23 due to slight differences in tune and the fact that the tracking plots have a coarser bin, that smears out fine structure. The width of the bands in these Figures indicates the amount of coupling (and varies with change in tune as seen by comparison of these figures). It becomes large when the chromaticity of the Booster is corrected to zero, indicated by our analytic and tracking results.

AGS - BOOSTER LATTICE
Averaged Emittance = $50\pi \text{ mm-mrad}$

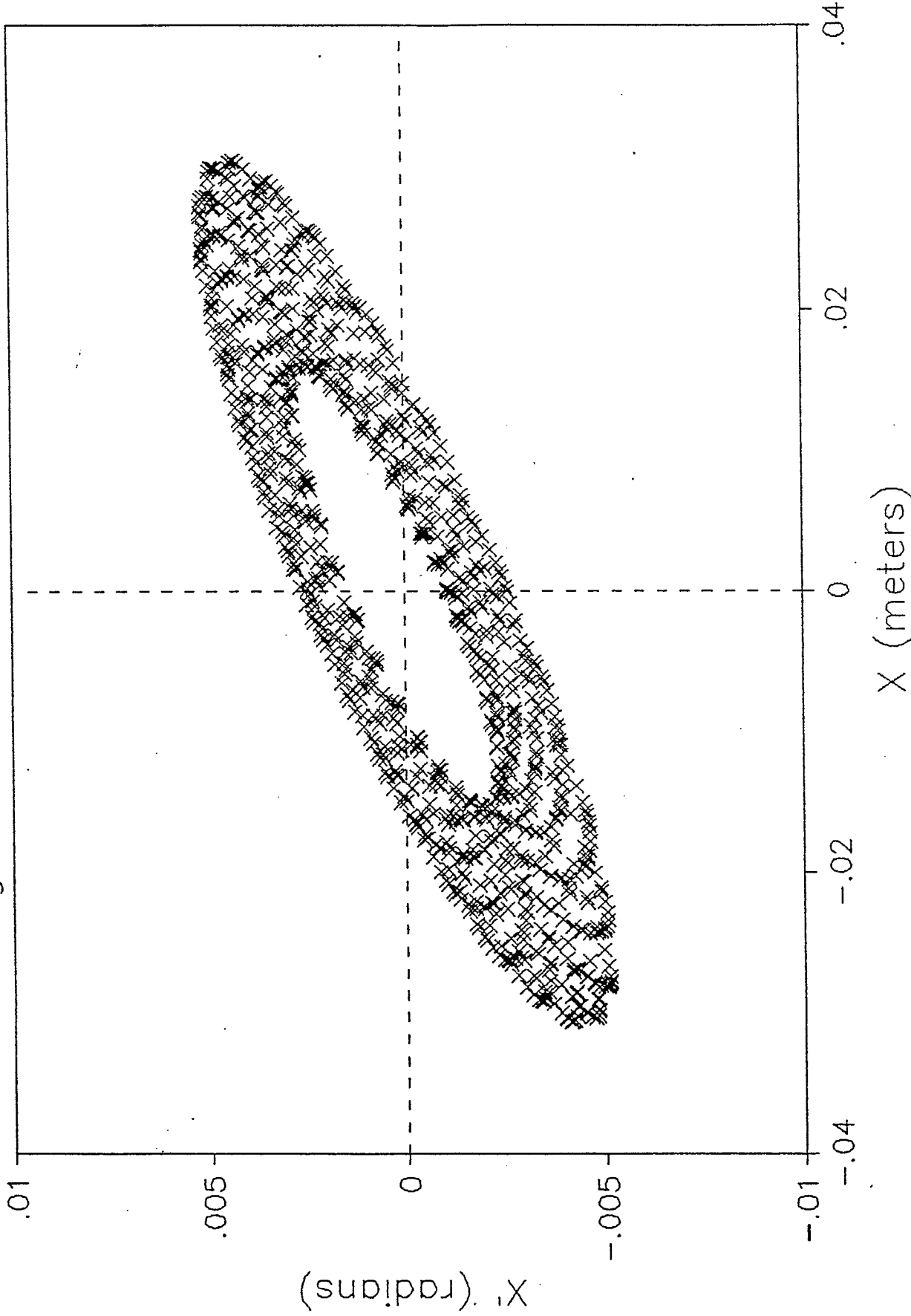


Figure 20: Shows the phase plot of (x, x') at chromaticity $C_x = C_z = 0$.

AGS - BOOSTER LATTICE
Averaged Emittance = $50\pi \text{ mm-mrad}$

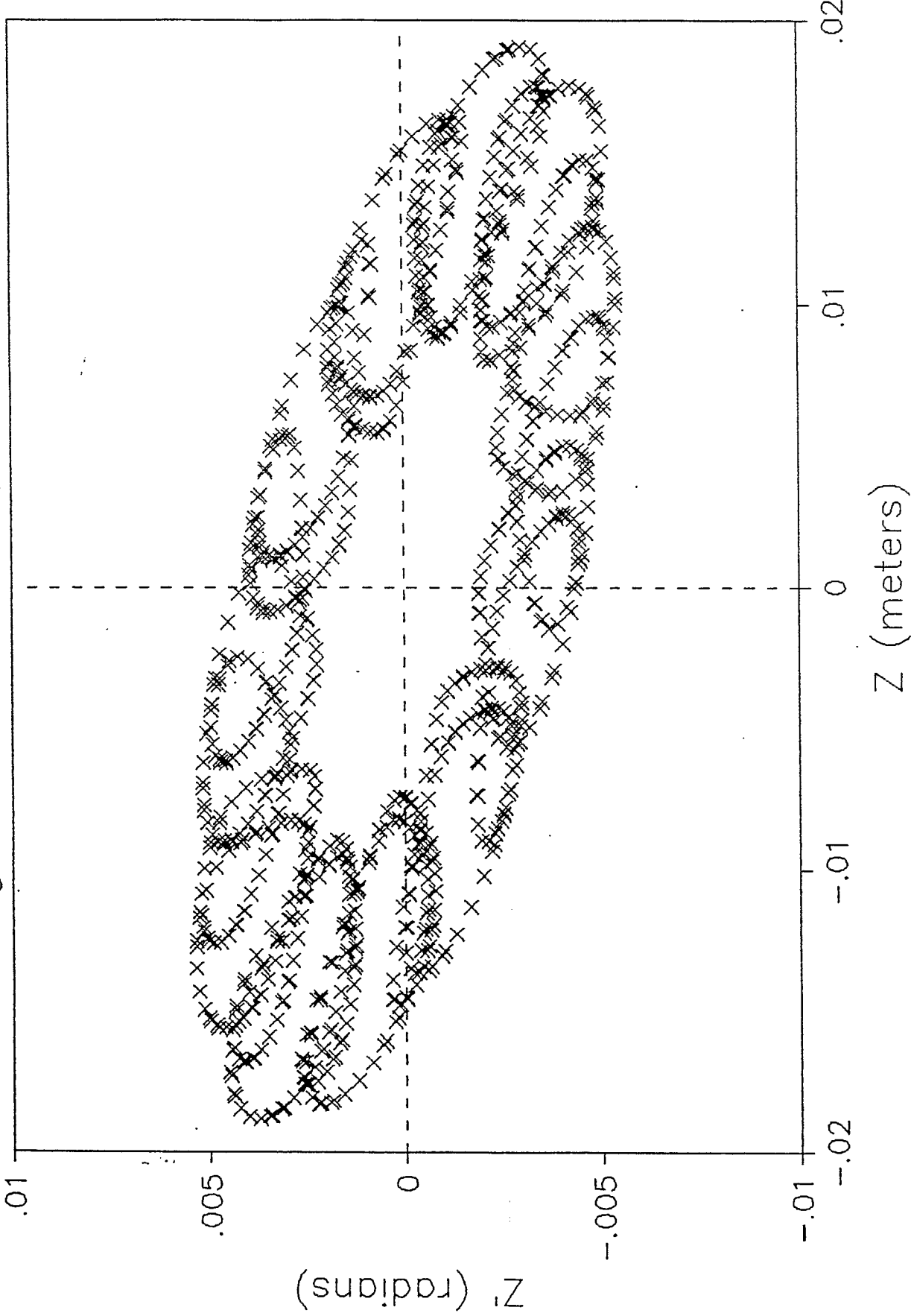


Figure 21 : Shows the phase plot of (z, z') at chromaticity $C_x = C_z = 0$.

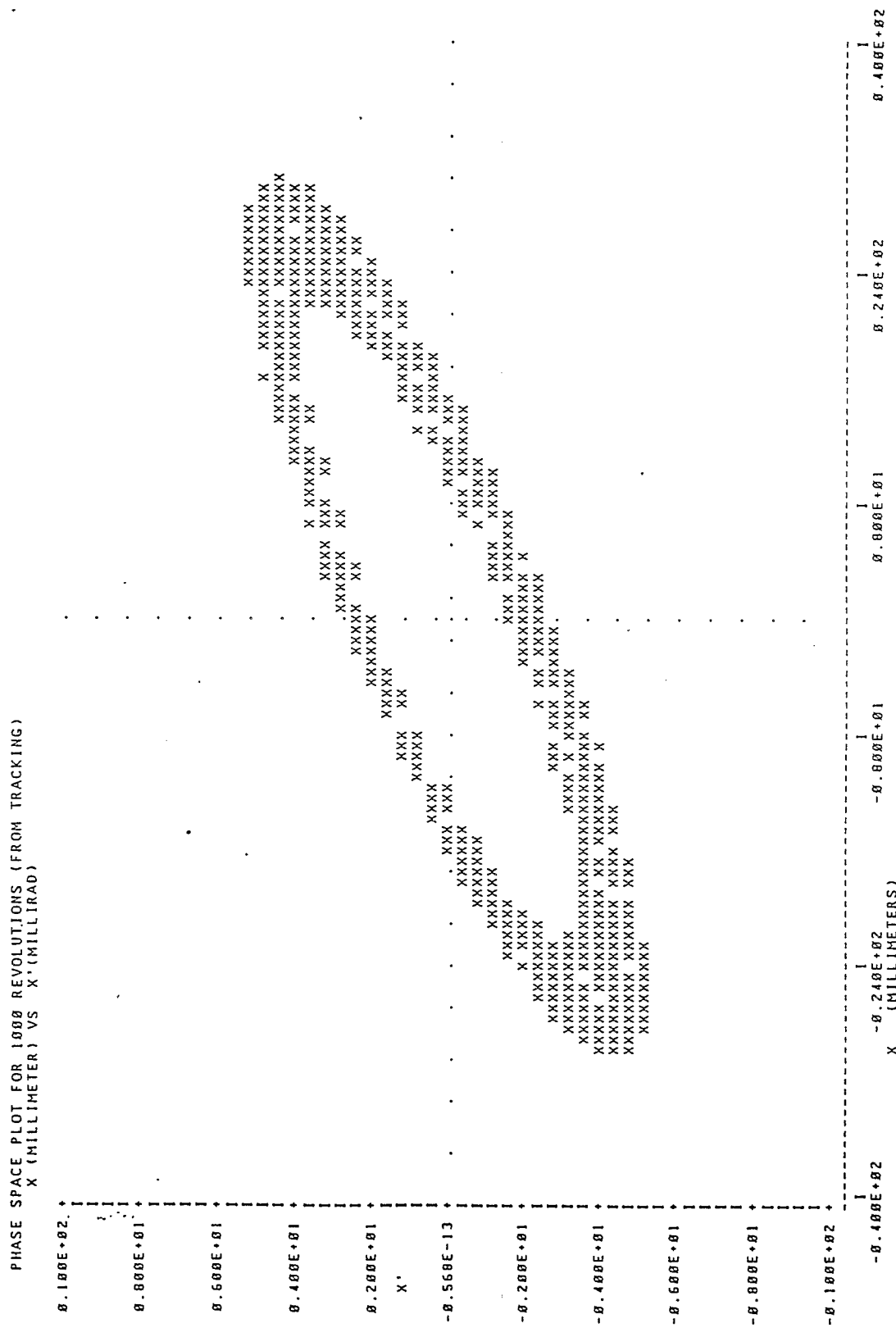


Figure 22: Shows the plot of (x, \dot{x}) , obtained from tracking (at chromaticity $C_{\chi^*} = C_{\tau^*} = 0$).

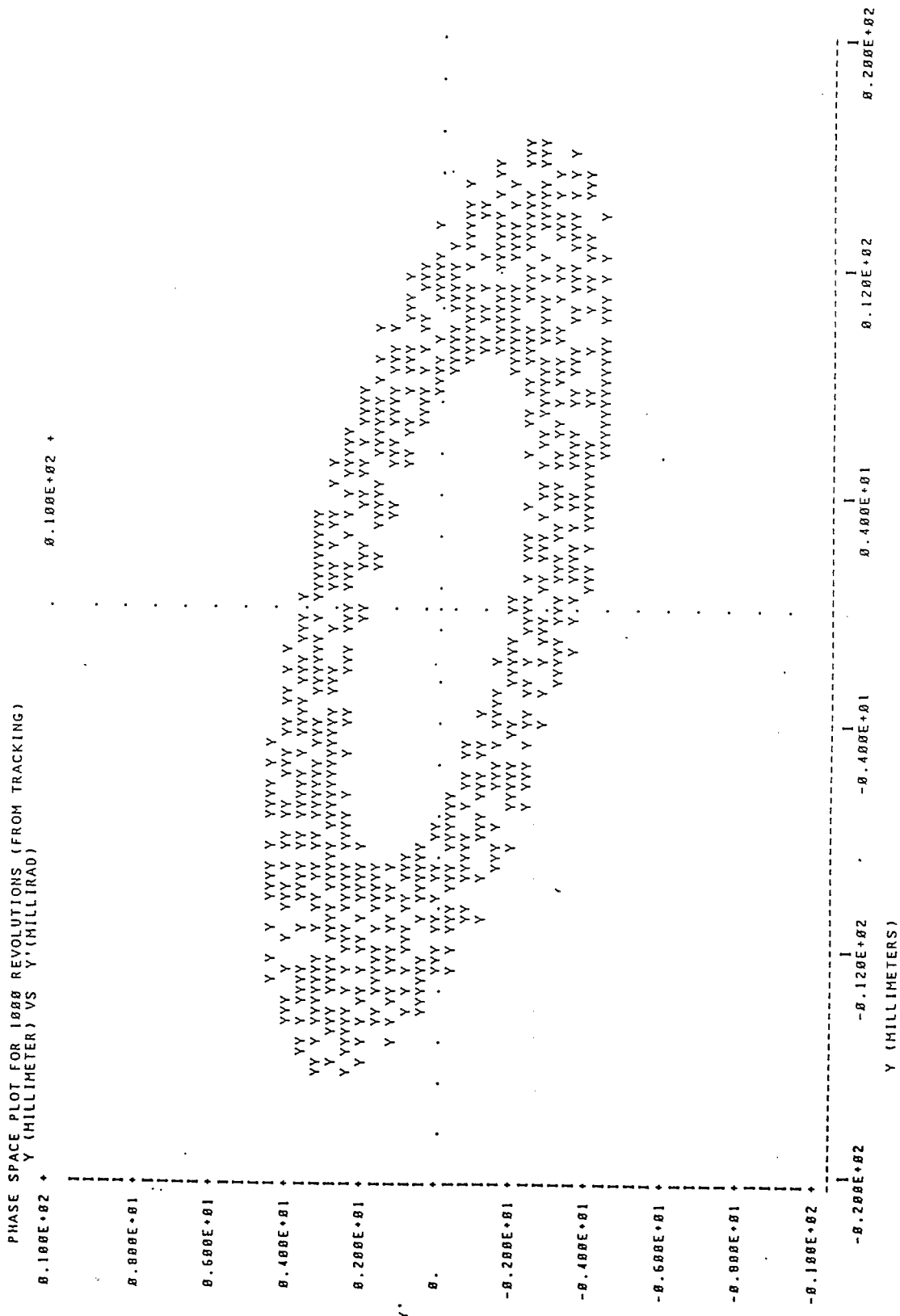


Figure 23: Shows the plot of (Y, Y') , obtained from tracking (at chromaticity $C_X=C_Z=0$).

AGS - BOOSTER LATTICE
Averaged Emittance = 50π mm-mrad

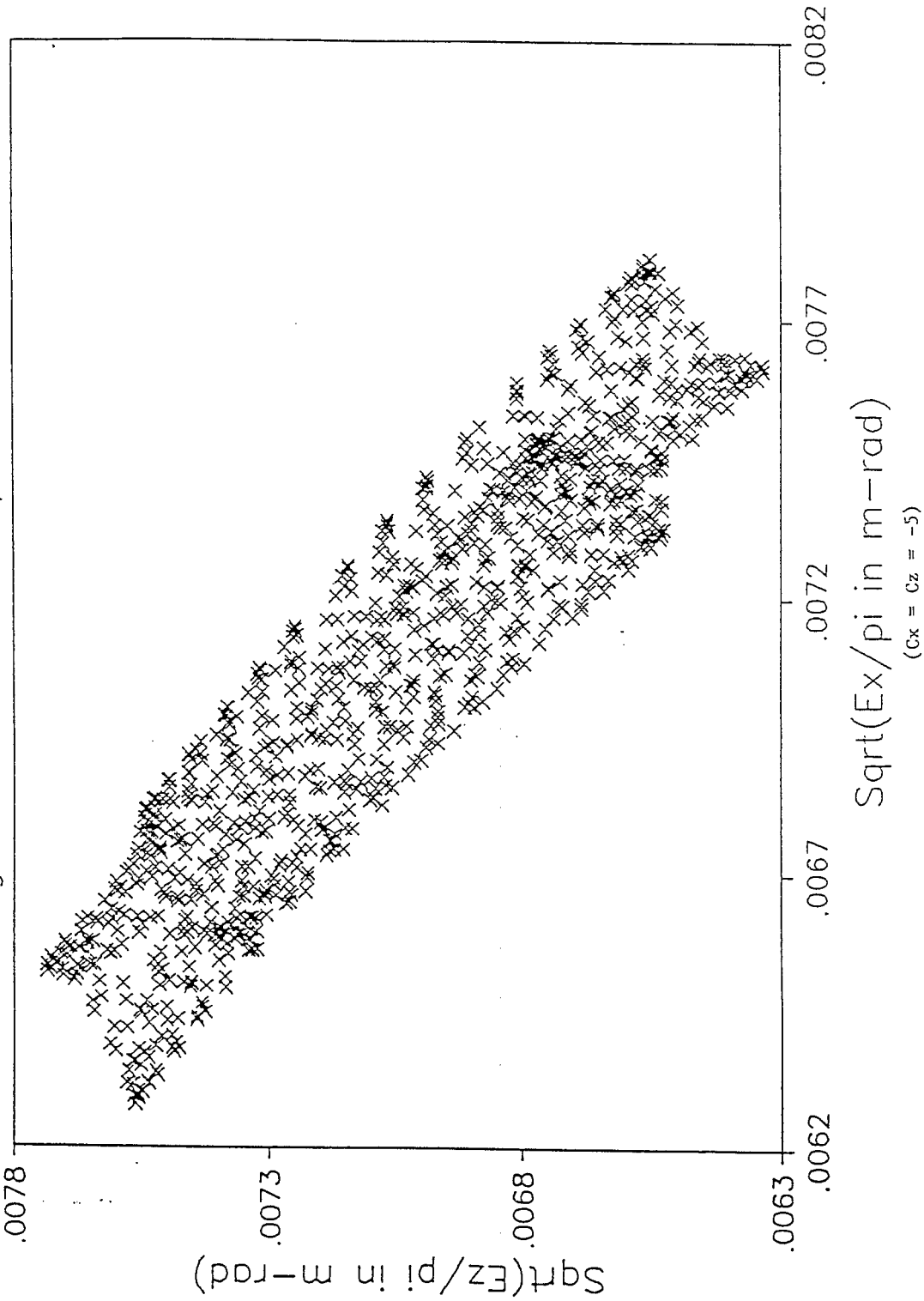


Figure 24: Shows the plot of $E_x^{1/2}$ versus $E_z^{1/2}$ for ($c_x = c_z = -5$).

Furthermore, comparisons of Figures 25 and 26 (phase plots of x, \dot{x} and z, \dot{z} respectively) which illustrates the reduction in the $(2\nu_x - 2\nu_z)$ coupling at chromaticities $C_x = C_z = -5$, with Figures 27 and 28 (obtained from tracking also with $C_x = C_z = -5$) again shows good agreement between our analytic and tracking results. (Noting a slight tune difference in tracking.)

AGS - BOOSTER LATTICE
Averaged Emittance = $50\pi \text{ mm-mrad}$

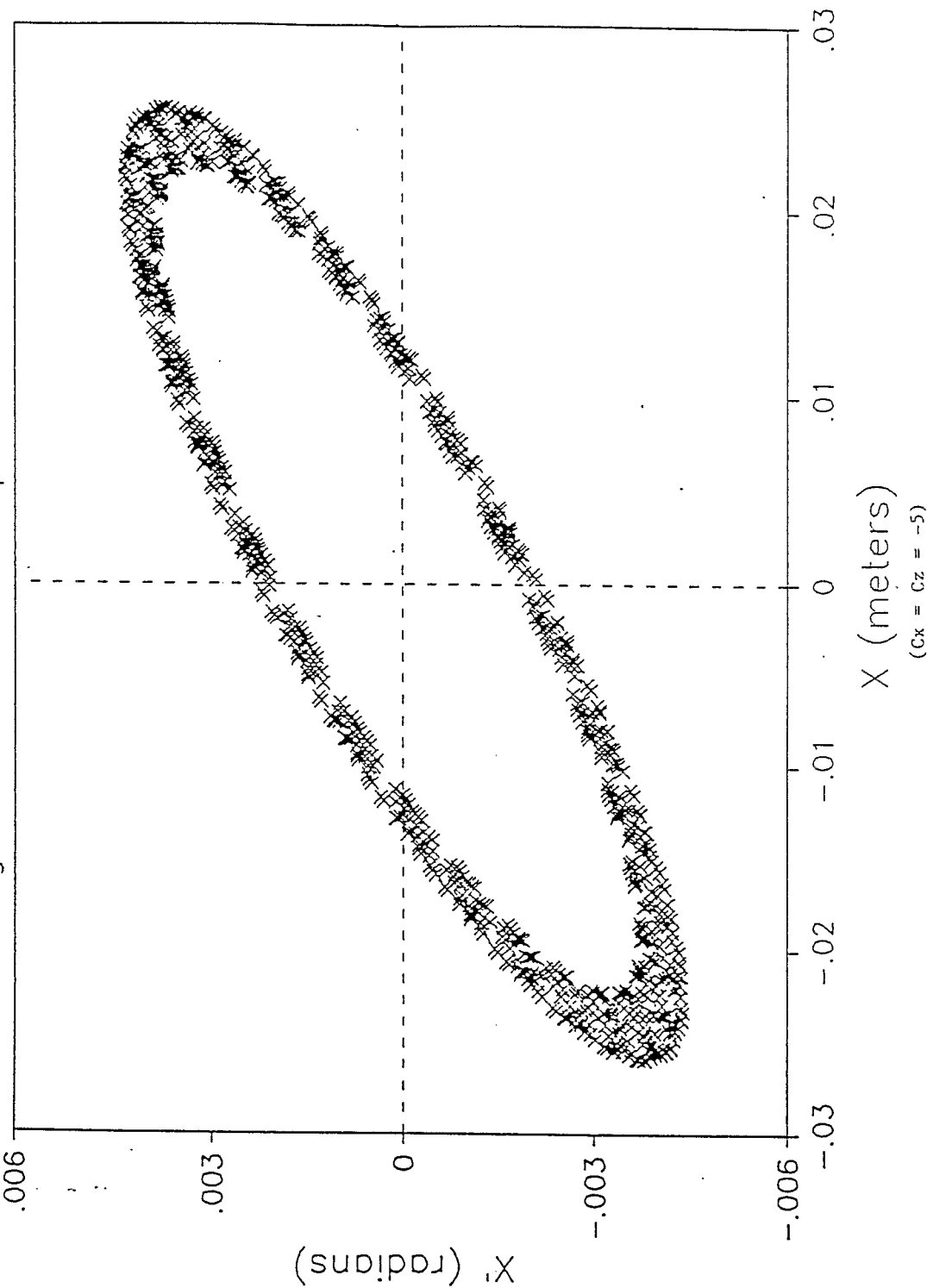


Figure 23 : Shows the plot of (x, x') at chromaticity $C_x = C_z = -5$.

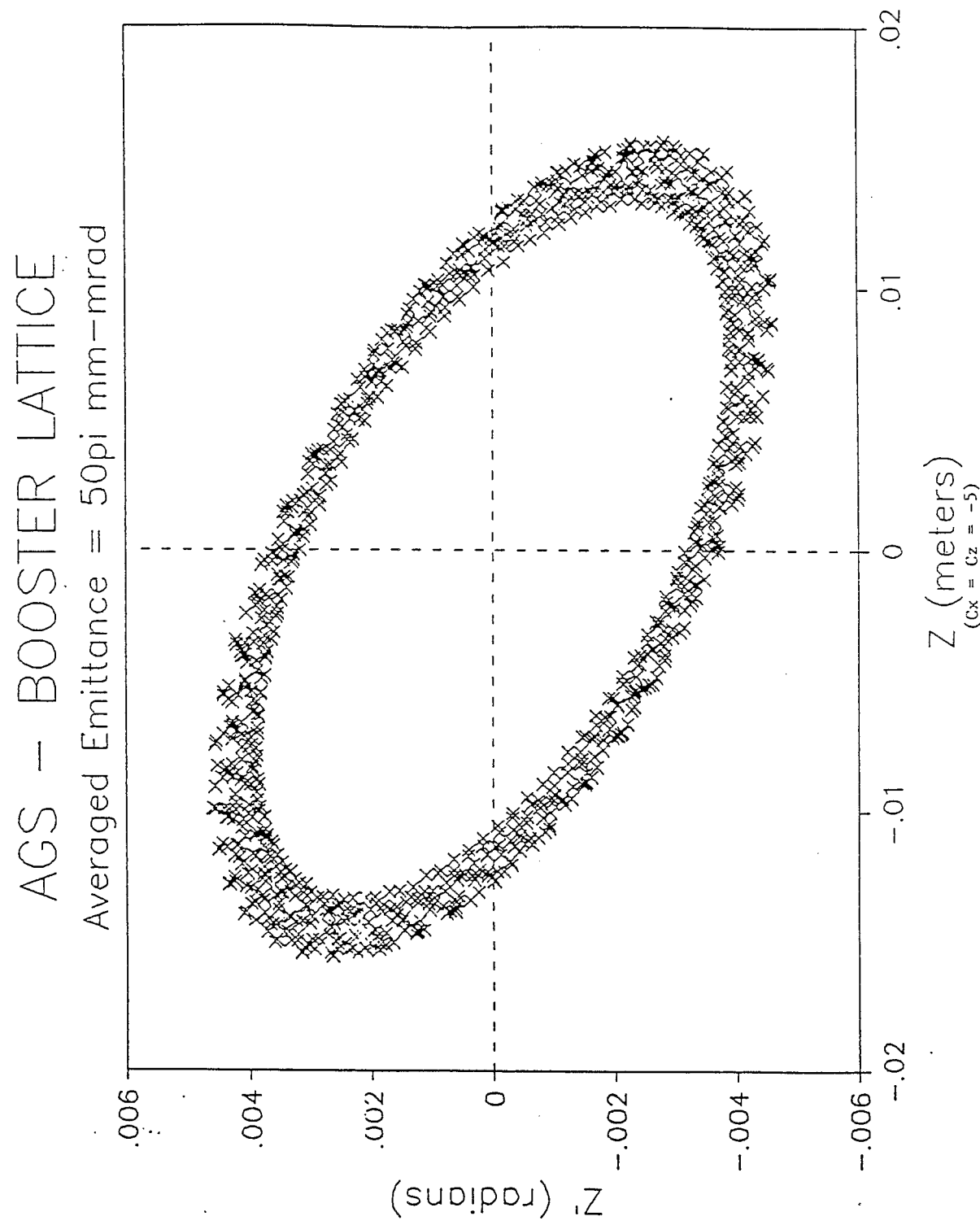


Figure 26 : Shows the plot of (z, z) at chromaticity $C_x = C_z = -5$.

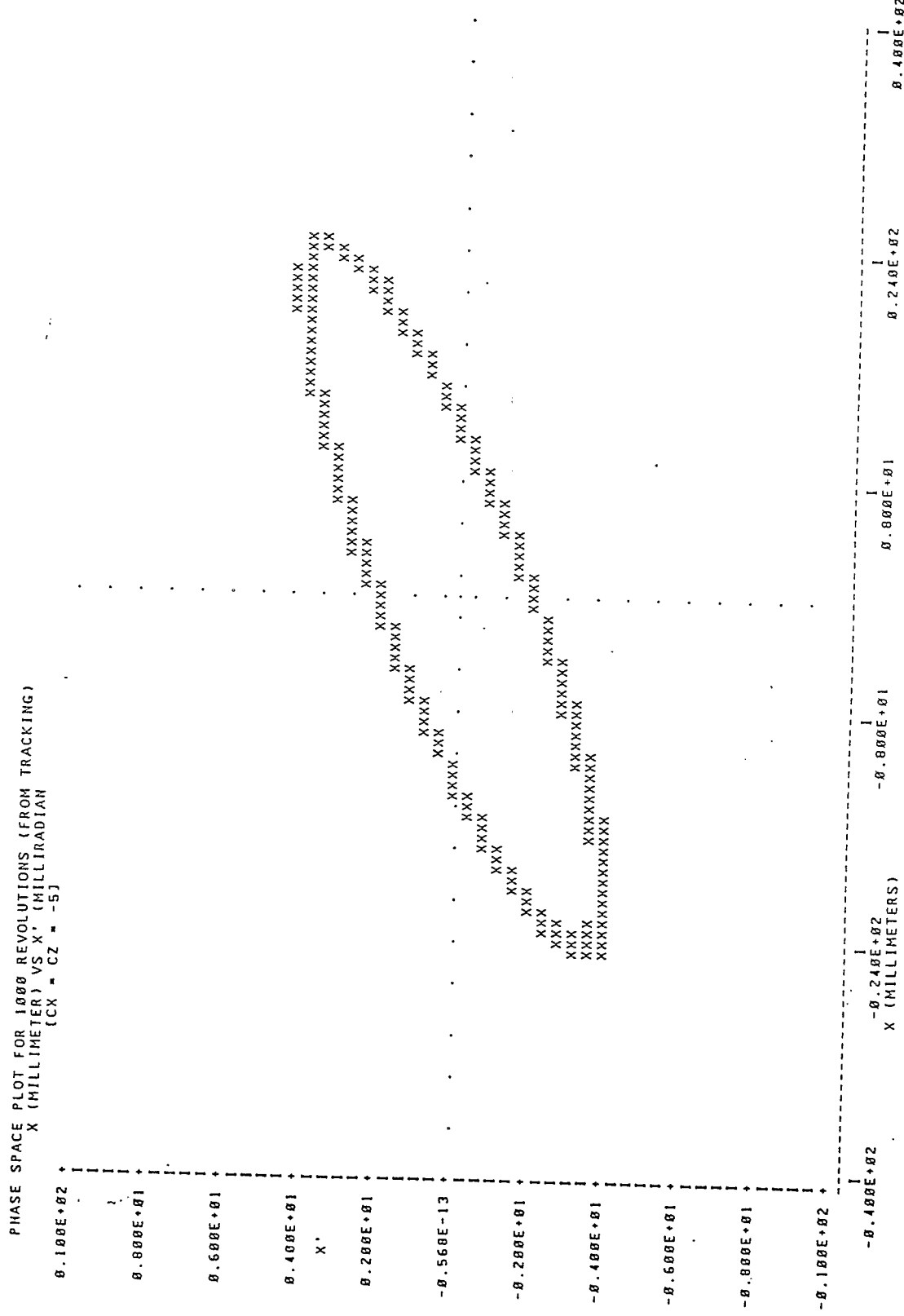


Figure 27: Shows the plot of (x , X) at chromaticity $C_x=C_z=-5$, (obtained from tracking).

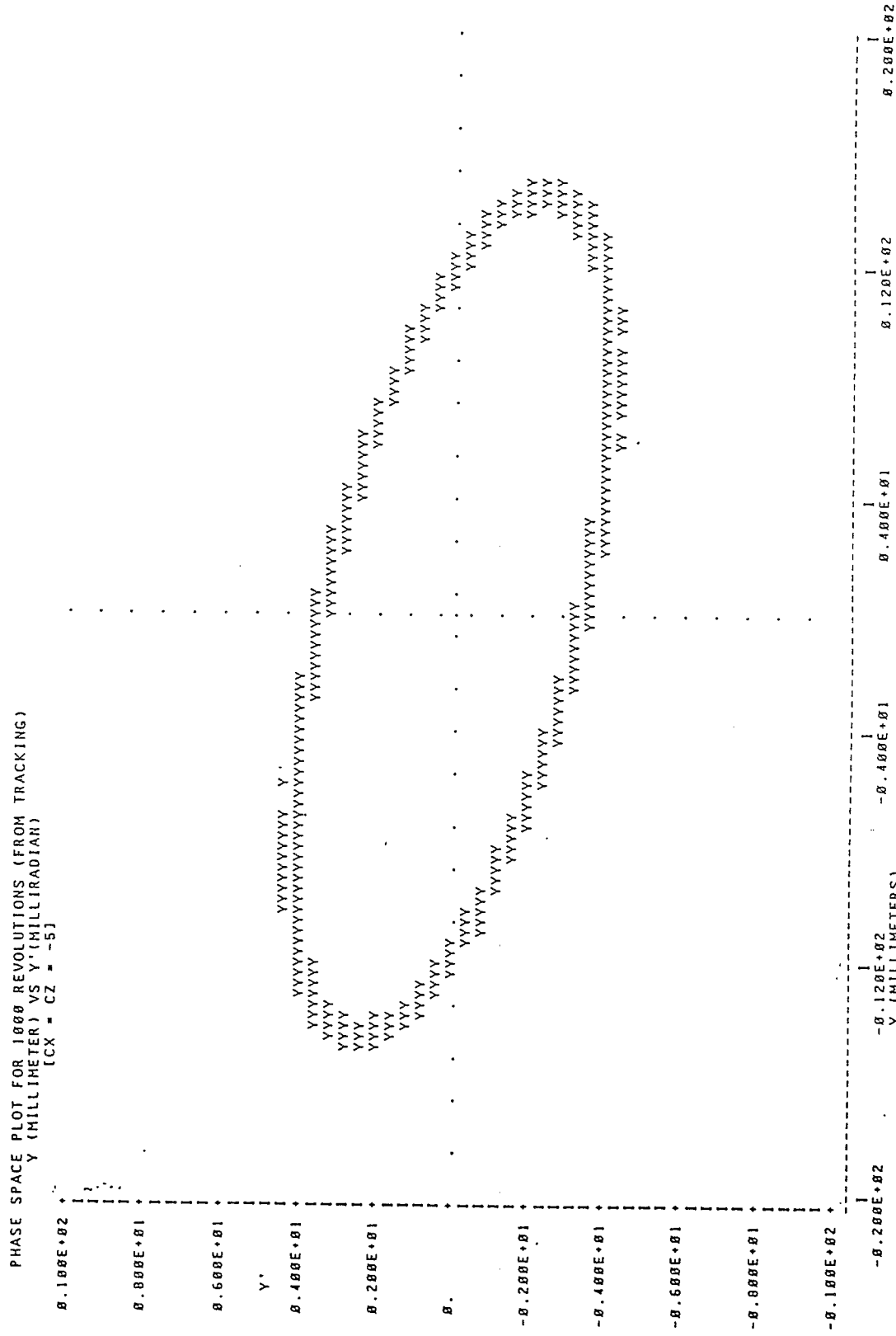


Figure 28: Shows the plot of (\cdot, \cdot) at chromaticity $C_X=C_Z=-5$ (obtained from tracking).

CONCLUSION

A large space charge tune shift in the AGS-Booster at injection, may cause the tunes to cross the fourth order structure resonances. If the space charge tune shift is large enough we may get near the third and sixth order resonances at tunes near 4.0. Tables I - III shows the perturbation to tunes and our results (e.g. stop bandwidths, resonance strengths for the third and fourth order resonances) obtained from NONLIN (Table II) and HARMON (Table III). Our analytic results agrees well with those obtained from tracking programs, if the initial conditions are considered. We note no preference for the choice of the initial tracking position. Since the maximum emittance growth will remain about the same regardless of the multipole position in the ring (Booster) from which we start the tracking. We also showed the existence of a chromaticity window for the Booster, where there is no $2v_x - 2v_z$ coupling. The size of the window would increase if either we decrease the total initial emittance and/or increase the number of the sextupoles per superperiod.

References

1. Z. Parsa, S. Tepikian, E. Courant, Second Order Perturbation Theory for Accelerators, BNL-39262
2. Z. Parsa, Proceedings of IEEE March 15-19, 1987, BNL-39449, 39450, 39451 and Accelerator Dynamics and Beam Aperture, BNL-38977
3. M. Donald, D. Schofield, A Users Guide to the HARMON Program, Lep Note 420 (1982); M. Donald, Private Commuication.
4. Z. Parsa, Booster Parameter List, BNL-39311; and Booster Design Manual
5. F. Dell, Tracking with modified 1980 version PATRICIA, (BNL) (unpublished) ; G. Parzen, Tracking with ORBIT, (BNL) (unpublished). The tracking results obtained by Dell and Parzen agreed qualitatively; F. Dell, private communication; H. Wiedemann, Chromaticity Correction in Large Storage Rings, PEP Note 220 (1976); H. Wiedemann, User's Guide for PATRICIA, PEP Tech. memo PTM-230 (1981); S. Tepikian, private communication.
6. Z. Parsa, S. Tepikian, Beam Behaviour Studies in Accelerators with Perturbation Theory, BNL-39454 (submitted to Particle Accelerator Journal)

T.N. DISTRIBUTION

BLDG. 911

AD Library
(H. Martin)
G. Bunce
R. Casey
H. Foelsche
J. Grisoli
P. Hughes (1) +
for each author
D. Lazarus
D. Lowenstein
T. Sluyters
W. Weng

BLDG. 902

D. Brown
J.G. Cottingham
P. Dahl
M. Garber
A. Ghosh
C. Goodzeit
A. Greene
R. Gupta
J. Herrera
S. Kahn
E. Kelly
G. Morgan
A. Prodell
W. Sampson
R. Shutt
P. Thompson
P. Wanderer
E. Willen

BLDG. 460

N. Samios
BLDG. 510
H. Gordon
T. Kycia
L. Leipuner
S. Lindenbaum
R. Palmer
M. Sakitt
M. Tannenbaum
L. Trueman

FOR SSC PAPERS

FNAL

W. Fowler
P. Mantsch

LBL

R. Donaldson (2)
W. Gilbert
V. Karpenko
P. Limon
K. Mirk
C. Taylor
M. Tigner

BLDG. 1005S

J. Claus
E. Courant
F. Dell
A. Flood
E. Forsyth
S. Y. Lee
Z. Parسا
G. Parzen
P. Reardon
S. Ruggiero
J. Sondericker
S. Tepekian

BLDG. 725

H. Halama

S&P in Magnet Division for all MD papers

S&P in Cryogenic Section for all Cryogenic Papers
(and J. Briggs, R. Dagradi, H. Hildebrand,
W. Kollmer)